Design of Cytostretch Skin

A human cell based stretchable, flexible and mass-producible skin tissue model for drug development

B.J. van Meer

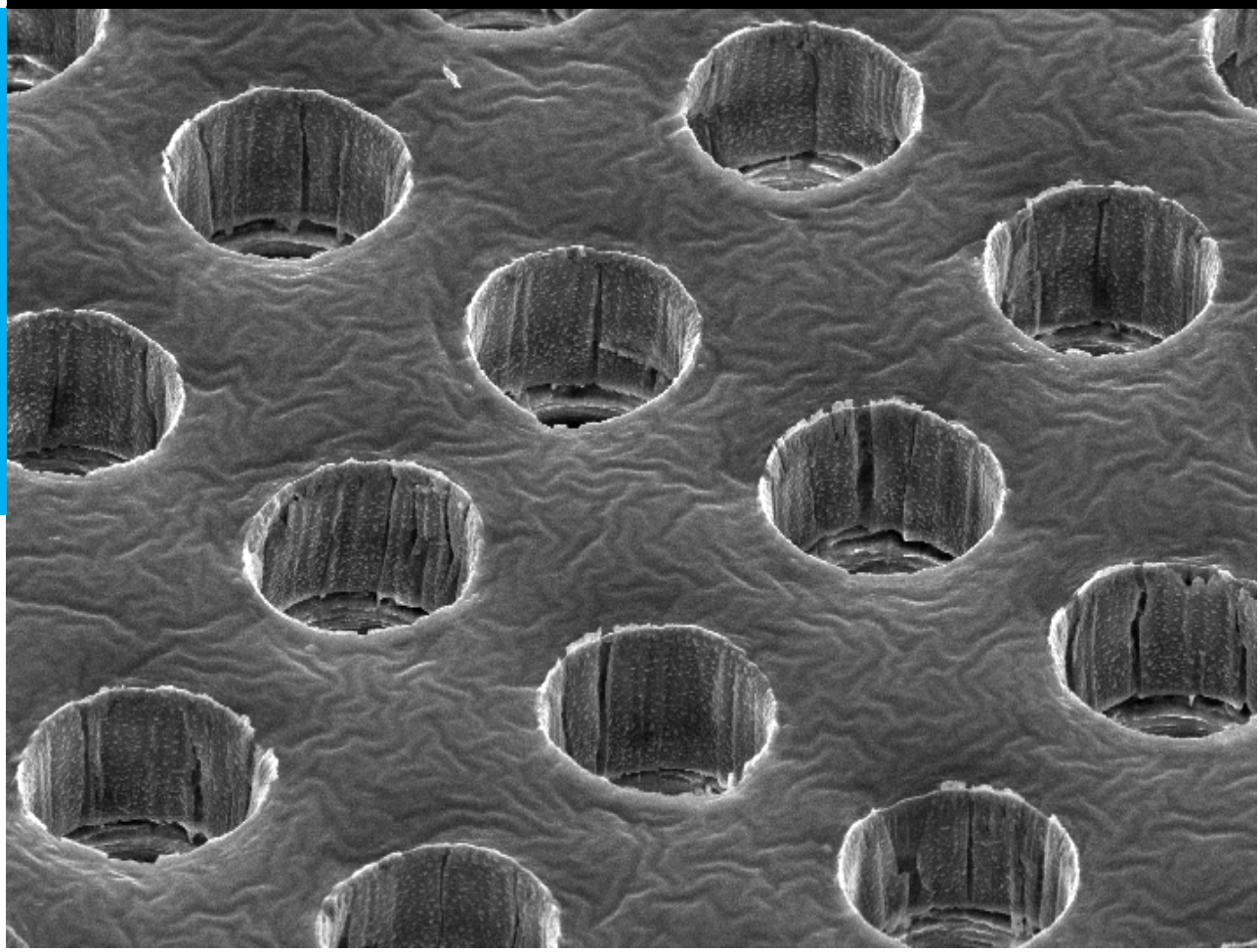

Delft University of Technology

TU Delft Delft University of Technology

Challenge the future

Design of Cytostretch Skin
A human cell based stretchable, flexible and mass-producible skin tissue model for drug development

By
B.J. van Meer

in partial fulfilment of the requirements for the degree of

Master of Science
in Electrical Engineering

at the Delft University of Technology,
to be defended publicly on Tuesday March 25, 2014 at 16:00

Supervisor:
Prof. Dr. Ir. R. Dekker
Thesis committee:
Dr. G. Pandraud
Dr. A. van de Stolpe
Prof. Dr. P.M. Sarro
Dr. J. Hoekstra

Delft University of Technology
Faculty of Electrical Engineering, Mathematics and Computer Science
Department of Microelectrical Engineering

Abstract

In the near future, human cell based Organ-on-Chip models are likely to replace animal experimentation during the development of new drugs. Not only is animal testing associated with ethical issues, but human cell based models can also give a more accurate representation of the human physiology, resulting in more reliable results of drug screening experiments. Furthermore, high-throughput drug screening is made possible by real-time readout of cell activity, using electrodes or other forms of cellular readout. Additionally, the high costs of drug development will be reduced, especially if the new devices will be suitable for mass production. To be able to accurately model the human physiology, the device must be fabricated using biocompatible materials, often polymers with special requirements like flexibility and stretchability. These materials are in general not standardized in microfabrication cleanroom environments, limiting the current designs suitability for mass production.

In this thesis an Organ-on-Chip device was designed, fabricated and validated for use in advanced skin tissue modeling. Without compromising for the requirements imposed by the physiology of skin tissue, the device is designed to be suitable for mass production. A prior model for cardiotoxicity screening, Cytostretch was used as a starting point for the skin model device. The new features added to the design were fabricated by adding certain steps to the manufacturing process, compatible with the current process flow. This modular approach makes the Cytostretch technology flexible and suitable to rapidly adapt the device design for modeling different tissues in the future. In this research, methods were explored for (i) the fabrication of large membranes, (ii) the fabrication of holes with a diameter of 5 to 8 μm, and (iii) the deposition of layers on polydimethylsiloxane (PDMS). As a result, large perforated membranes of PDMS were fabricated and a new etching technique for PDMS was developed in order to create the small feature size of maximally 8 μm in the membrane. Also, a novel method to prevent thermally induced stress in layers deposited on PDMS is presented. After fabrication of the device, it has been validated to be suitable for skin tissue engineering by culturing human dermal tissue on the device.

Contents

Chapter 1

Introduction

In recent years, the merge of the fields of microelectronic fabrication and biomedical sciences uncovered numerous novel and unexplored research areas. The demand for a new generation of devices with (electro)mechanical stimuli for cell-based organ models requires the use of flexible and biocompatible materials, which are often not standardized in microfabrication. In this thesis a new design of a human skin model is proposed, built and tested using a newly developed processing technique for one of the most promising materials for Organ-on-Chip models: polydimethylsiloxane (PDMS).

In the first Section of this Chapter Organ-on-Chip is introduced, and more specifically the Cytostretch model; a previously developed Heart-on-Chip model which will be the starting point for the skin model. Polymers, like PDMS, are often an essential part of Organ-on-Chip models and in the second Section a short overview is given of the problems associated with polymer processing. In the last Section the scope of this thesis is defined.

1.1 Organ-on-Chip

One of the most valuable and promising research areas involving microelectrical and biomedical engineering is Organ-on-Chip. In Organ-on-Chip simplified models of human organs are made using a microfabricated device [32]. The recently developed iPS technology allows *in vitro* culturing of well defined and reproducible human tissue with a certain gnomic profile [62]. Research is in an early stage and while the replacement of donor organs might be possible in the far future, these models are currently valuable for the development of new drug compounds and as drug screening devices [22]. Studies have shown that *in vitro* human stem cell based models are in some cases already more accurate than animal models [11]. If these models would prove to be superior compared to animal models at all times, the latter will be replaced shortly, as this will resolve ethical issues and will be cost efficient, since mass production is possible. In this Section

the superiority of human cell based models compared to animal models is discussed, with an example of a cardiotoxic drug where the toxicity was not detected with the use of animal tests, and which had to be withdrawn from the market after causing numerous deaths.

1.1.1 Vioxx, a killer medicine

In 1999, the pharmaceutical company Merck introduced a new arthritis drug after approval by the Food and Drug Administration (FDA): Vioxx. The success of the drug was enormous, resulting in more than 84 million prescriptions worldwide and 2 million daily users on September 30, 2004, which was the date that Merck voluntarily withdrew Vioxx from the market [44]. The drug turned out to induce hearth attacks and strokes; estimations of the death toll vary from 50,000 (FDA) to 500,000 [56]. Although critics are of a different opinion, the court ruled that Merck did not know about the side effects of the drug before going to market. Since a large part of drug testing is being done on animals, the resulting data can often not be translated to human patients.

Even without the horrifying death toll figures, the consequences of a withdrawal of a drug from the market are vast. Before a drug is admitted to the market, its producing company has invested on average 800 million USD in development. Such investment, together with severe reputational damage, decline in stock value and liabilities, make the financial impact of a withdrawal enormous. A more reliable detection method for toxicity in an early phase of the development path of drugs, would thus not only improve safety for patients, but would also make economical sense for pharmaceutical companies.

Testing on animals is expensive and associated with ethical issues, plus animals do not model the human physiology well enough to accurately test for toxic effects of drugs when these are used on humans. As a step towards more reliable cardiotoxicity screening the Cytostretch model was developed. Cytostretch is a model based on human cells that will be explained in more detail below.

1.1.2 Cytostretch for cardiotoxicity

To accurately model human organs using human cells, current cell culture infrastructure is not sufficient. Currently, for cardiotoxicity screening human heart muscle cells are plated on a Multi-Electrode-Array (MEA) or characterized using patch clamp techniques. Although both techniques have their own specific advantages and applications, these techniques have downsides as well.

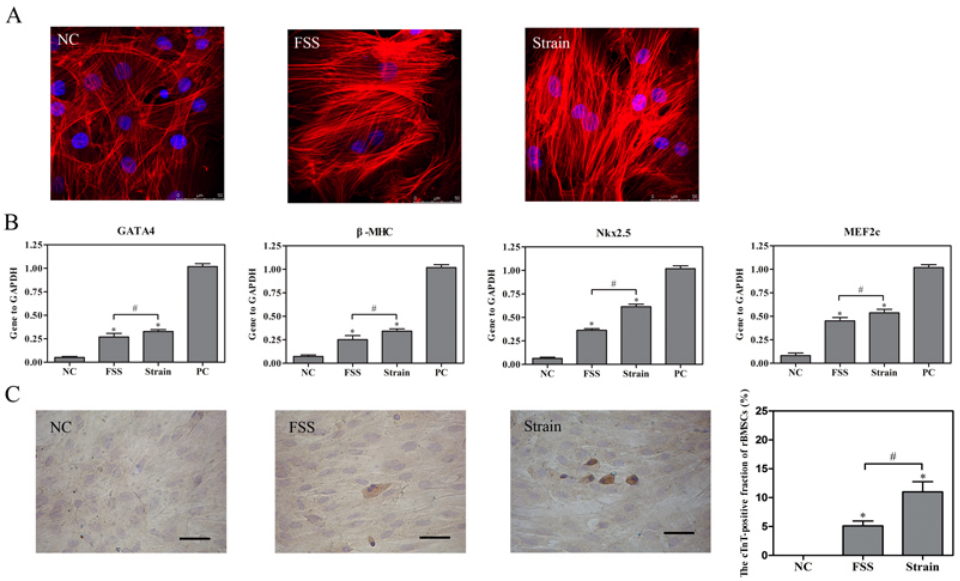

Figure 1.1: Fluid shear strain and mechanical strain increase the expression of proteins that are associated with the maturation of heart muscle cells: GATA4, β-MHC, NKx2.5 and MEF2c. *Image cited from [31].*

These two techniques are incomparable to the physiological conditions in the human body. To be more precise, the cells do not mature enough due to of a lack of repeated mechanical strain (Fig. 1.1) [31], and the cytoskeleton of the cells shows elongated fibers due to the rigid substrate (Figure 1.2) [60].

Cytostretch was developed by Delft University of Technology in collaboration with the Leids Universitary Medical Center and Philips Research to address these problems and to create a more physiologically correct environment for the heart muscle cells to mature, resulting in a more reliable heart model. Cytostretch is a stretchable multi-electrode array, made in silicon with polydimethylsiloxane (PDMS) as the flexible substrate for the cells. The low Young's modulus (750 - 4000 kPa [1], [24]) of PDMS makes that this material is soft enough to prevent elongated fibers of the cells, and its elasticity is well suitable for repeated mechanical straining of the heart muscle cells. Within the PDMS, thin and stretchable interconnects of titaniumnitride connect the electrodes in the center of the device with the bond pads on the edge of the device. Additionally, microgrooves in the PDMS membrane promote the alignment of the cells in a predefined direction. Cytostretch has been fabricated in two different layouts: the circular design, and the dog bone design (Figure 1.3a and 1.3b). When the PDMS membrane of the circular Cytostretch is inflated by a small backside air pressure, the cells plated on top on the membrane will experience strain in al directions. The dog bone design on the other hand, allows for

Figure 1.2: A heart muscle cell on a glass plate shows stressed fibers due to the hardness of the substrate. *With courtesy of Stefan Braam (Pluriomics).*

straining of the cells in the direction perpendicular to the length of the device [47], this feature together with the possibility to align the cells in a particular direction, makes it possible to unidirectionally strain the cells. The fabrication process flow of the device is discussed in detail in Chapter 3.

After the cells are cultured and subjected to repeated mechanical strain, which results in maturation of the cardiac cells, drug screening tests can be started. During the experiments, the Cytostretch device measures the extracellular field potential of the heart muscle cells (cardiomyocytes) that are plated on the flexible membrane. Drug compounds can be added to the culture medium, in order to investigate whether they produce a change in the extracellular field potential of the cardiomyocytes, possibly indicating heart failure. Additionally, the membrane can be inflated above the regular value to mimic increased cardiac activity.

Although many different organ models have emerged over the past few years [8, 14, 27], Cytostretch is one of the most advanced systems due to its biocompatible microelectrodes and microstructured surface for cell alignment, as well as its fabrication technology. While many devices are cumbersome to manufacture and require many manual manipulations which are

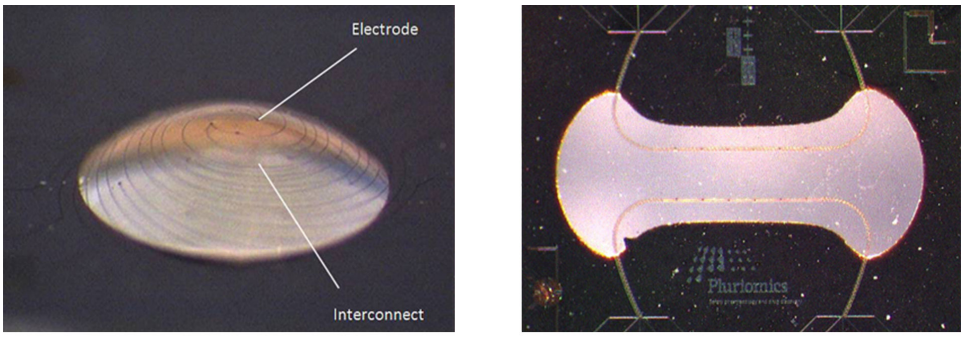

(a) (b)

Figure 1.3: The two different layouts of Cytostretch: (a) the circular design and (b) the dog bone design.

likely to introduce process variations which compromises the reproducibility and increases the price, Cytostretch is fabricated in a highly controlled microfabrication cleanroom environment and is inherently suitable for mass-production. This enables high-throughput cardiotoxicity screening, a significant cost reduction, and more reliable batch-to-batch results, all of which are required before pharmaceutical companies will embrace the Cytostretch technology and governmental administrations will approve it as a substitute for animal experiments.

1.2 Polymer processing

For standard microfabrication materials such as common metals, silicon, silicon dioxide, silicon nitride, etc., processing techniques are well established. Since most polymers found their way into the cleanroom not that long ago, processing of these materials is not straightforward. Many processing techniques like deposition, etching, cleaning and patterning are still unoptimized compared to the processing of standard microfabrication materials, resulting in limitations on minimum feature size, process repeatability and mass production. Also, handling these materials in a cleanroom environment can contaminate other fabrication processes, as some of the polymers give off particles if not treated correctly. As a result, many process facilities are reluctant to introduce polymer processing. Therefor developing stable standard processes is crucial for the future development of Organ-on-Chip.

1.3 The scope of this thesis

The current fabrication method for the Cytostretch device resolves polymer processing issues by introducing the polymer in the end of the process, but this might not be possible when new features are added to the device. New

features have to be developed to make the Cytostretch platform suitable for other Organ-on-Chip models. Stretching, measurement of the extracellular field potential and aligning cells can be done using the original Cytostretch, however, other organ models may require additional features. To be able to meet the requirements for different organ models in the future, the fabrication process will be made modular by including or excluding features just by adding or leaving out process steps during the fabrication of the device. The assignment of this Masters project was to (i) incorporate a module or modules in the existing process flow to meet the requirements for using Cytostretch as a Skin-on-Chip model, (ii) including building a prototype and (iii) validating the device.

The requirements for an accurate and reliable skin model will be discussed in the next Chapter.

Chapter 2

Skin models for drug development

In 1898, Ljunggren made the first attempt to store human skin outside of the body and ever since numerous efforts have contributed to the highly developed field of *in vitro* skin culturing. Being of utmost importance for patients with severe burn injuries, developing skin grafts for clinical applications has been a major area of focus. As a result many skin grafts nowadays come from skin cultures, either from the patients own cells or donor cells. Another application of skin tissue engineering is *in vitro* drug screening, aiming to improve screening accuracy and to make it more affordable as compared to drug screening on animals. There are also less ethical constraints associated with the use of *in vitro* tissue models. Although skin tissue engineering has come a long way, there are still some hurdles to overcome before the cultured tissue resembles the skin well enough to ensure accurate modeling of the *in vivo* situation.

A short background on human skin is presented in the first section. The following sections discuss the current *in vitro* skin models and their future improvements.

2.1 Skin

In order to model or reproduce human skin tissue it is important to understand the crucial functions and features of the skin. Skin, representing approximately 16% of the total bodyweight, is the largest organ of the human body. It is the first line of defense against injuries, infections, viruses and parasites. Besides being a physical barrier and being indispensable for the regulation of the body's temperature, skin is also an active immune organ that has biochemical instruments to fight intruding microorganisms. Furthermore, the skin has important metabolic functions in the production of certain proteins (e.g. vitamin D) [59].

The anatomy of skin is complex. Light microscopy and immunohistochemistry are frequently used tools to study the anatomy of *in vitro* engineered tissue samples, in order to evaluate whether it resembles the *in vivo* situation. The skin is a two-layered organ (Fig. 2.1) with varying thickness over the body. The top layer is called the epidermis and is a rapidly renewing layer of keratinocytes, in progressive stages of differentiation, from the inner layers to the surface of the skin. Keratinocytes are cells that get cornified when they reach the most differentiated stage, resulting in the tough outer layer of skin. The second layer of the skin, the dermis, is the thickest part of the skin, constituting about 95% of the total weight of the skin. Dermis consists of two sublayers, the upper layer of which (papillary dermis) is thinner and very elastic. The deeper reticular dermis is thicker and exists of, amongst others, bloodvessels, nerve endings, lymphatics and also epithelial cell sources for intradermal structures, such as sweat glands and hair follicles. Together these layers make the skin almost impenetrable, robust and very regenerative [5, 59].

Immunohistochemical staining of a cross section of healthy human skin shows this layered structure clearly (Fig. 2.2). The largest part is pink, indicating the dermis. In the dermis some different cell nuclei (purple) are found, some of which are dermal fibroblasts. Also some vascular tissue can be seen, but the most important part is the transition to the epidermis. At this interface a large number of nuclei can be seen, which are the keratinocytes. They gradually differentiate toward more cornified cells that in the top part of the cross section form the outer skin layer. A comparable structure in the cross section of an engineered skin tissue is one of the most important indications that it is physiological correct.

While most dermal cells have a fixed position in the skin, there is an important cell type that migrates from the blood vessels underneath the skin through the dermis and the epidermis. As these *Langerhans cells* are indispensable guardians of the immune system in the skin, these cells are key to the development of an accurate skin model.

2.2 Current *in vitro* skin models

Current skin grafts are made out of cells of the two layers that were identified in the previous section: epidermal keratinocytes and dermal fibroblasts. The fibroblasts make a feeder layer that acts as dermis. Many different types of substrates or scaffolds, such as collagen gel, sponges and biodegradable polymers, can be used as a support layer for the fibroblasts. A commonly used example is MatriDerm®, which is a collagen based substrate in which the fibroblasts are seeded before keratinocytes are plated on top. It is shown that the addition of certain additional cell types, such as endothelial cells,

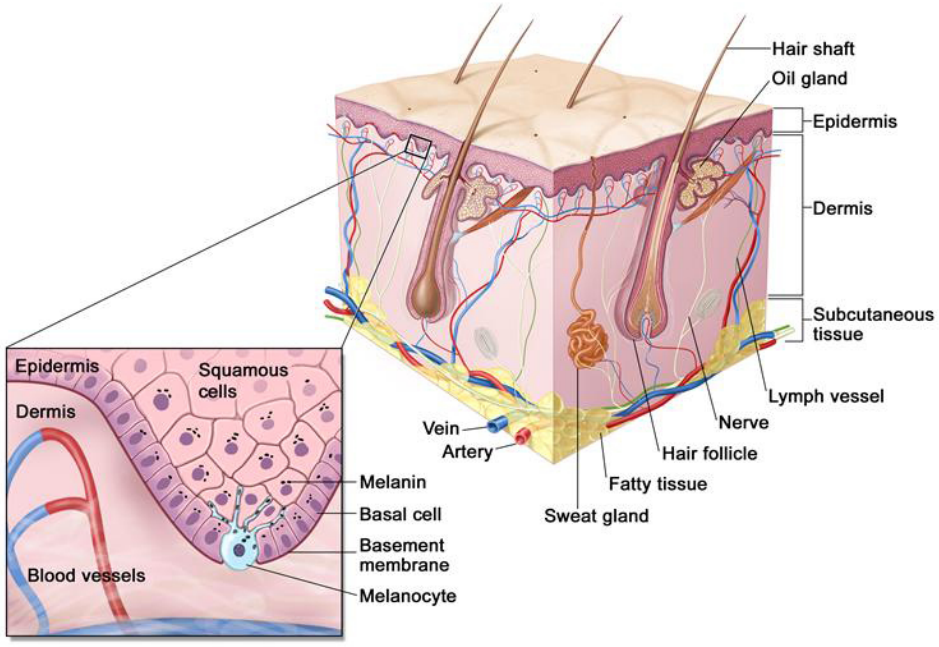

Figure 2.1: Schematic cross section of human skin (©Terese Winslow).

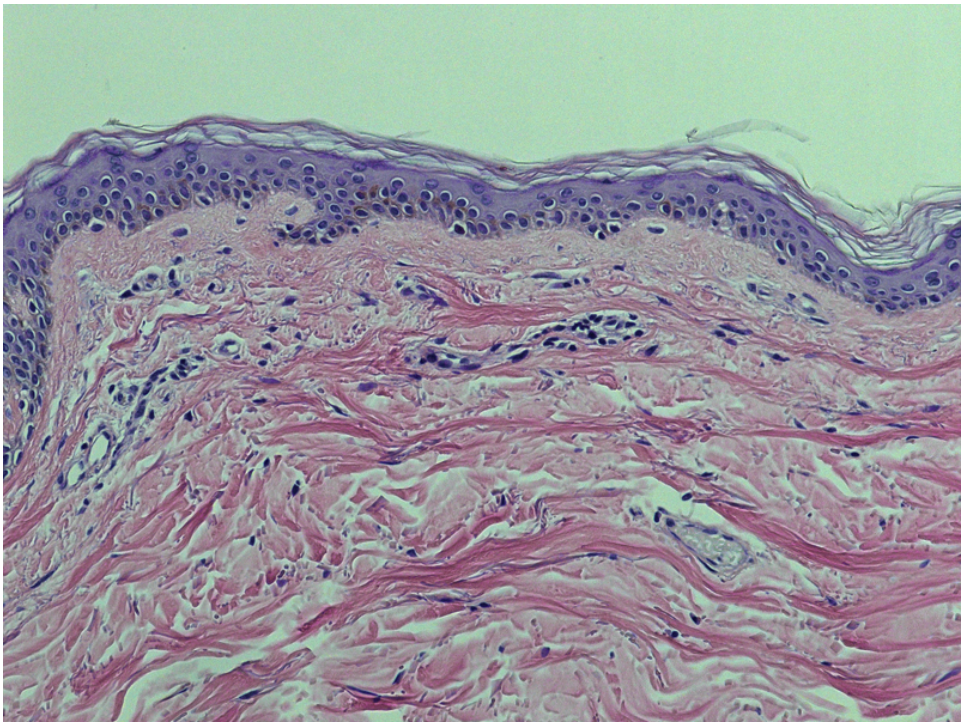

Figure 2.2: Immunohistochemical staining of a cross section of healthy human skin. *With courtesy of Taco Waaijman (VUmc).*

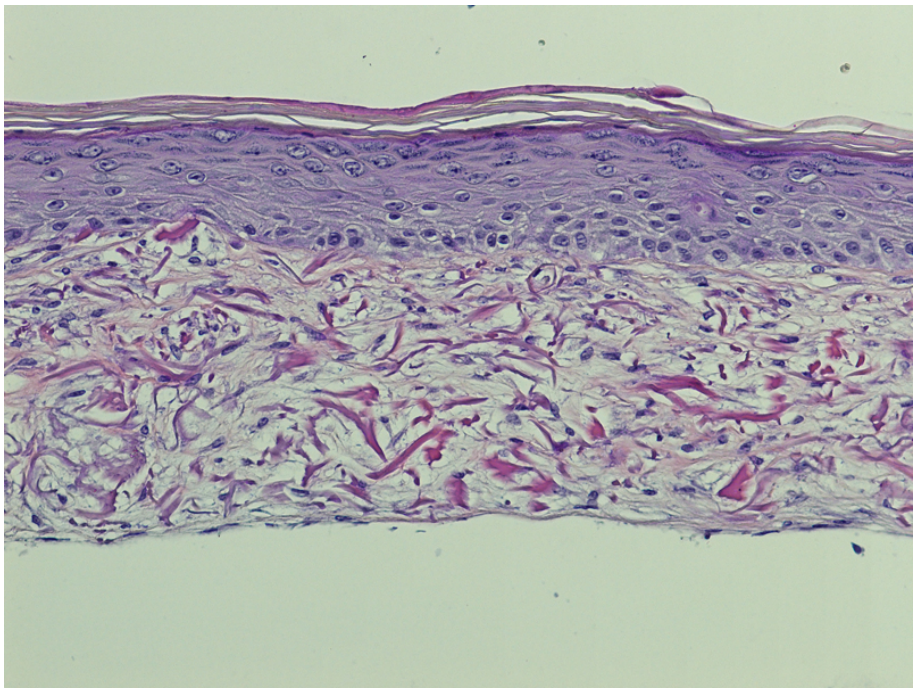

Figure 2.3: Immunohistochemical staining of a cross section of *in vitro* engineered skin tissue on MatriDerm®. *With courtesy of Taco Waaijman (VUmc).*

can make the skin models even more physiological correct by adding sources for (faster) vascularization [2].

The immunohistochemistry and the expressed proteins of current cell cultured grafts indicate that these constructs are not completely matured skin tissue, since they show features associated with healing or hyperproliferative tissue [6, 53]. Due to the robust and regenerative character of *in vivo* skin, *in vitro* developed skin grafts for the treatment of patients do not have to be perfect. Certain metabolism that stimulates further growth of the engineered tissue will take place in interaction with a patient's skin as soon as the graft is applied, and thus immature and near-complete skin tissue suffices. Although this immaturity of the skin graft does not impose a problem for the treatment of patients, this issue is necessary to be resolved to ensure an accurate *in vitro* skin model for drug testing.

Figure 2.3 shows the immunohistochemical staining of a cross section of an *in vitro* engineered skin tissue on a MatriDerm® substrate. The dermis is clearly visible as the bottom part of the cross section and although less precise as in Fig. 2.2, the interface between the dermis and epidermis is visible with a row of aligned nuclei. Further towards the top of the tissue, the keratinocytes become more differentiated and they result in the outer skin layer.

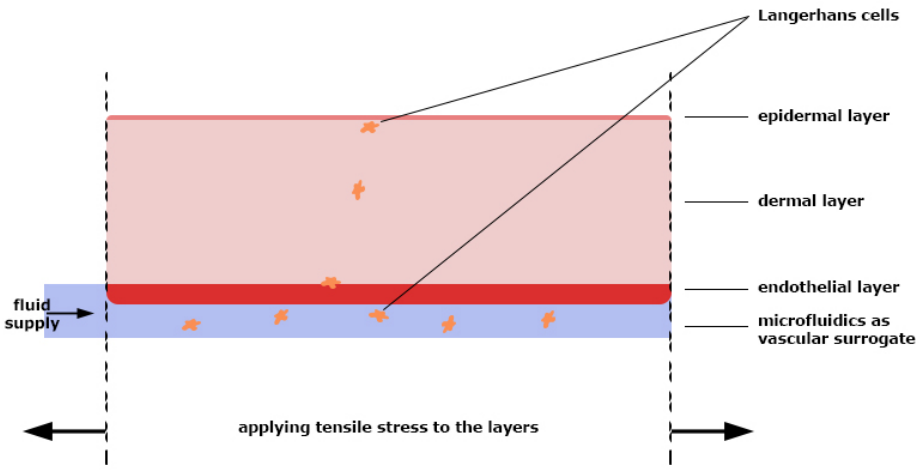

Figure 2.4: Schematic cross section of the improved skin model.

2.3 Improving current *in vitro* skin models

To ensure correct proliferation and differentiation of cells *in vitro* is one of the most challenging tasks, not only when developing skin tissue, but for cell cultures of any organ in general. Many factors influence the growth and differentiation of cells inside the human body, and replicating this is complex. Several chemical factors have been identified, but it has been shown that mechanical stimulation also has influence on the proliferation and differentiation of cells [31, 35, 54]. Some cells experience a constant cyclic mechanical deformation in the human body, for example due to beating of the heart and inhalation of the lungs. Clearly, a model organ should replicate such deformations. Although skin is not subject to cyclic or periodic deformation, it is strained continuously due to a persons movements and its interactions with the environment. Proper skin models must replicate these mechanical deformations, as they do not only play an important role in the differentiation, but might also influence the interaction with chemical compounds [50].

As indicated in the Section 2.1, including Langerhans cells would also improve the model significantly. When added to the culture medium, they should be able to migrate from one layer to another. A microfluidic channel could act as a vascular tube in the model, in order to supply the culture medium to the tissue. A layer of endothelial cells on the inside of the vascular channel should be included to promote vascularization in the dermis, and the possibly the migration of Langerhans cells.

To conclude, our improved model should ideally have three layers of cell types, from top to bottom: epidermal, dermal and endothelial cells. Langerhans cells should be introduced from the culture medium through a

microfluidic channel, in direct connection with the endothelial cell layer, and the Langerhans cells should be able to migrate through all layers of the skin equivalent. A schematic cross section of such a model is shown in Fig. 2.4.

In the next Chapter a new Cytostretch design is derived from the original Cytostretch model, which fulfills the necessary requirements for the improved skin model.

Chapter 3

Design of Cytostretch Skin

The development of Cytostretch was started in 2009 in a collaboration between Delft University of Technology, Leiden University Medical Center and Philips Research. The aim was to develop a mass-producible, stretchable microelectrode array for cardiotoxicity drug screening. Complex issues in microfabrication, such as biocompatibility, access to inversed microscopic inspection and surface treatment for protein adhesion were resolved [7, 41, 47]. Also solutions have been found for technological challenges, such as stretchable electrodes, making the design a good starting point for the development of the new skin model.

To improve the current skin models as described in the previous Chapter using the Cytostretch technology, extended process flows for the fabrication of Cytostretch are proposed at the end of this Chapter. Because fabrication of the design has to be compatible with the process flow of the current Cytostretch device, the key steps of this process will be explained in the next Section.

3.1 Current process flow of Cytostretch

Since the processing of polydimethylsiloxane (PDMS) is not straightforward, using it as a substrate to make features like electrodes is complex, if not impossible and introduces many technological difficulties [7]. The process flow developed for the fabrication of Cytostretch is adapted to cope with these issues. The process flow introduces the polymer only at the end of the fabrication sequence: the 'polymer-last approach' [18]. This approach fabricates features with standard silicon process technologies and materials, on standard silicon substrates, and afterward transferring these structures to the PDMS, hereby allowing the fabrication of fine pitch structures in the stretchable membrane. Key to this approach is to build the device upside down, which makes the last added layer (i.e. PDMS) the substrate (the membrane) of the resulting device (Fig. 3.1). The detailed process flow of

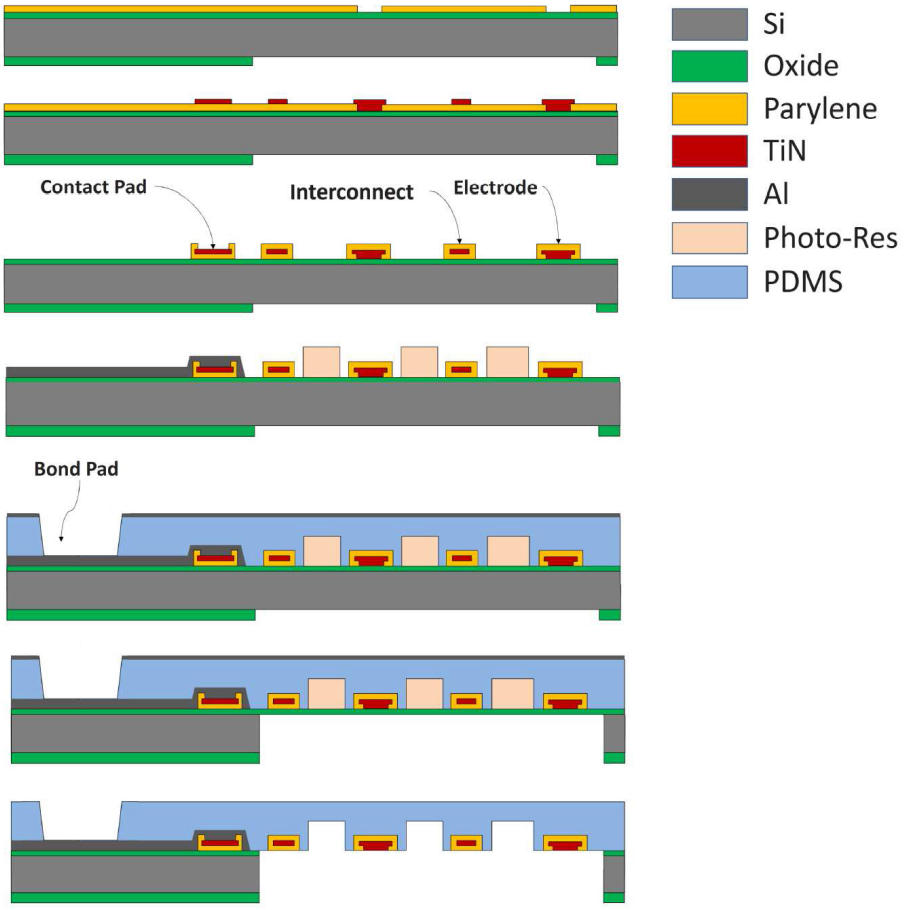

Figure 3.1: Current process flow of Cytostretch [45] using the polymer-last approach.

Cytostretch is discussed in [45, 47].

The process flow of the current Cytostretch model consists of three key elements: fabrication of microelectrodes and interconnects, fabrication of alignment grooves, and release of the membrane. The latter is required for making a PDMS membrane, however the first two can be considered modular and the process steps to build them can be included or excluded without affecting other features of the device. The interconnects are made out of titaniumnitride (TiN), isolated by a layer of parylene. The grooves are fabricated by making pillars of photoresist (photo-res) that act as a mold for the PDMS layer. The photoresist is removed after the silicon substrate is

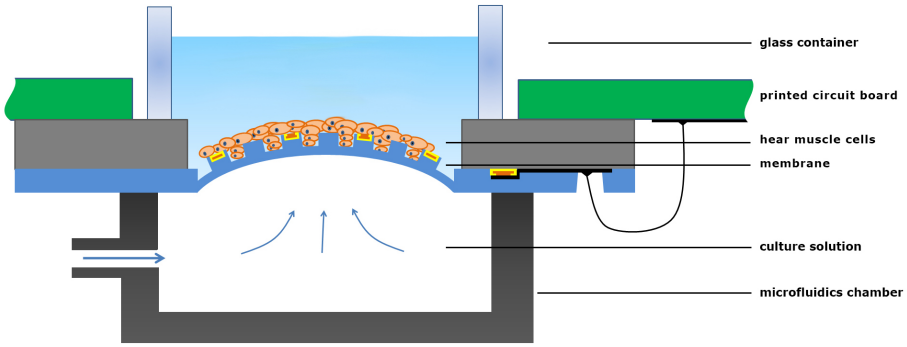

Figure 3.2: Active Cytostretch device for cardiotoxicity screening [45].

removed by etching. After separation of the silicon chips, a plexi glass ring to contain the medium is glued to the backside of the chip. This assembly is clamped to a printed circuit board (PCB), which holds a small pressure chamber to inflate or deflate the membrane, and two small electrical spring connectors. The latter contact the chip on the front side and connect the electrodes to contact pads which are located on standard positions on the PCB, so the total device can be tested in a standard MEA reader (Fig. 3.2).

3.2 Device design

As discussed in the previous Chapter, the Cytostretch device for improved skin modeling is quite different from the device discussed in the previous Section. First of all, it consists of not one, but three layers of cell types, all of which should be accessible for the Langerhans cells from the culture medium. The culture medium must be supplied from underneath the device, which means it is only in direct contact with the endothelial cells. This can be done by replacing the air pressure chamber in Fig. 3.2 by a microfluidic channel. Inflating or deflating the membrane can now be done by controlling the flow and the pressure in the microchannel. If the microfluidic control system is part of the culture setup and not built into the device, such as with the air pressure chamber, the bottom of the membrane is accessible for cell plating before the device is placed in the setup and as a result can be coated with endothelial cells. However, when the dermal and epidermal layers are plated on top of the membrane it is impossible for both layers to have interaction with the endothelial layer, let alone that it would be possible for Langerhans cells to migrate from the culture solution to the dermis or epidermis. To overcome this problem the membrane needs to be

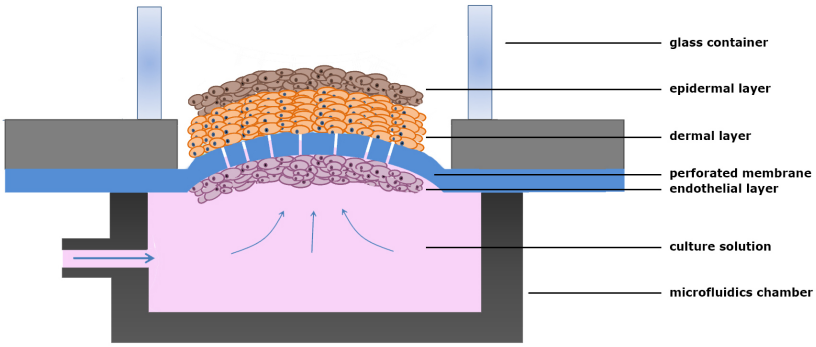

Figure 3.3: Design of Cytostretch Skin.

perforated. The holes should be large enough to allow Langerhans cells and chemical compounds to migrate, but need to be too small for other cells to fall through. Typical dermal fibroblasts are 10 to 15 μm in diameter [23], but they do not have a fixed morphology and can adapt their shape to some degree in order to migrate through narrow openings in the human body. The limitations to their dimensions are not known exactly, but from experience in the research group of Sue Gibbs in the VU Medical Center, the requirements are specified as half of the size of the fibroblasts: 5 to 8 μm.

For now, it is sufficient to have a membrane with holes to satisfy the requirements for an improved skin model, thus fabrication of grooves and microelectrodes is not a priority at this point. However, since current *in vitro* engineered skin tissue is relatively large in order to handle of this tissue when analyzing it using - for example - immunohistochemistry, it is necessary to increase the size of the membrane of the Cytostretch model. The membrane should have a diameter of at least 10 mm to meet the requirements.

In summary, to fabricate the Cytostretch model suitable for skin modeling, microgrooves and electrodes can be omitted and the additional design requirements for the adaption of the Cytostretch model device are

- a perforated membrane with a hole diameter in the range of 5 to 8 μm;
- a membrane diameter of at least 10 mm;
- cell plating possible on both sides of the membrane.

The proposed design of the Cytostretch Skin is depicted in Fig. 3.3.

3.3 Proposed process flows

In this Section, three process flows to fabricate the previously proposed design for the Cytostretch Skin model are discussed, all of which are modular compatible current process flow. PDMS patterning being as challenging as it is, different options should be tested and evaluated. The different techniques to pattern PDMS, their drawbacks and their constraints, are discussed in more detail in the next Chapter. In general there are two ways to pattern or structure a material: by depositing the material selectively (additive technology) or by removing the material selectively (subtractive technology). Suitable process flows are proposed for the additive technology, the subtractive technology, as well as a combination of the two. To demonstrate the modular character of the fabrication of the holes, the most extensive process flow is presented, including fabrication of microelectrodes, grooves and holes. The impact of the additional process steps in terms of extra photolithographic mask steps is also evaluated, since the number of mask steps is an indication for the cost and complexity of the process.

3.3.1 Selectively removing PDMS

In the process flow depicted in Fig. 3.1, PDMS is selectively removed to open the bond pads. A logical option would be to use this step to fabricate the holes in the PDMS membrane (Fig. 3.4). No extra mask steps or layers are required in this case.

3.3.2 Selective deposition of PDMS

In the process flow depicted in Fig. 3.1, PDMS is already selectively deposited to make grooves in the substrate. Similarly, a layer of photoresist thicker than the layer of PDMS can be used to fabricate the holes in the PDMS (Fig. 3.5). Since the grooves need to be fabricated with a different height, an additional mask step is required.

3.3.3 Selectively applying and removing PDMS

Finally, both techniques described above can be combined (Figure 3.6) to make holes in the PDMS. As with the first scenario, this would not introduce an additional mask step. The etch time is hereby reduced since the PDMS has to be etched open until the photoresist cast is reached. The photoresist is later removed with acetone.

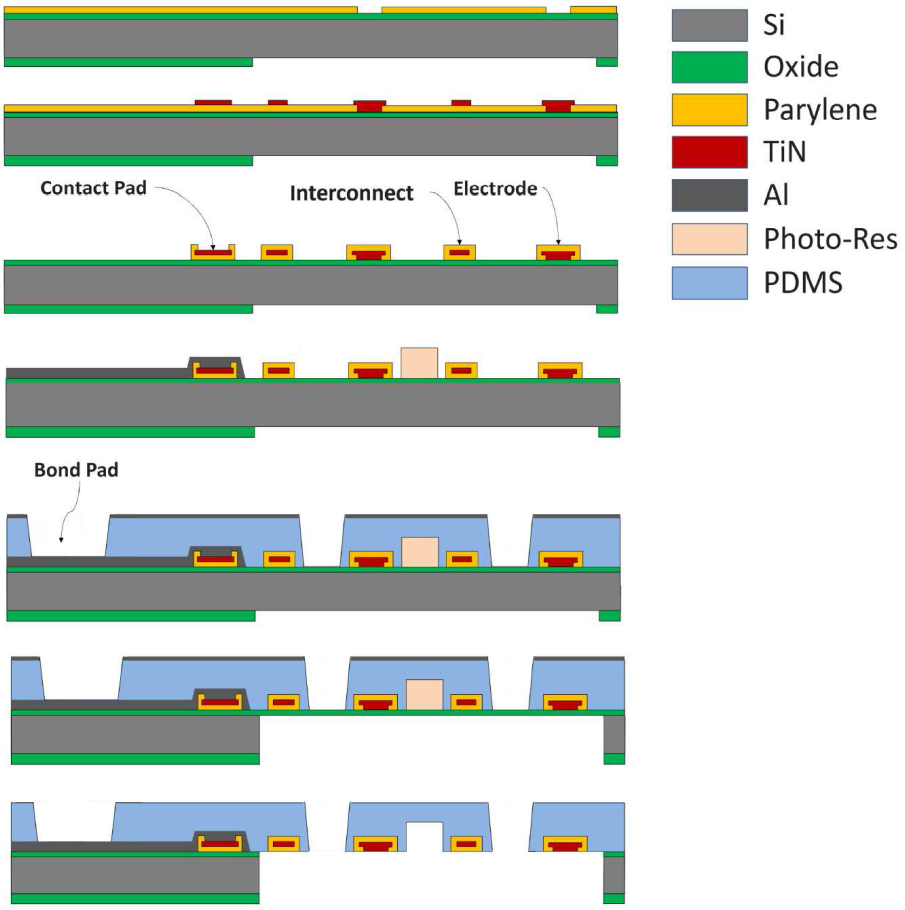

Figure 3.4: Selective removal of PDMS to fabricate holes. No extra mask steps are required. *Drawing adapted from [45].*

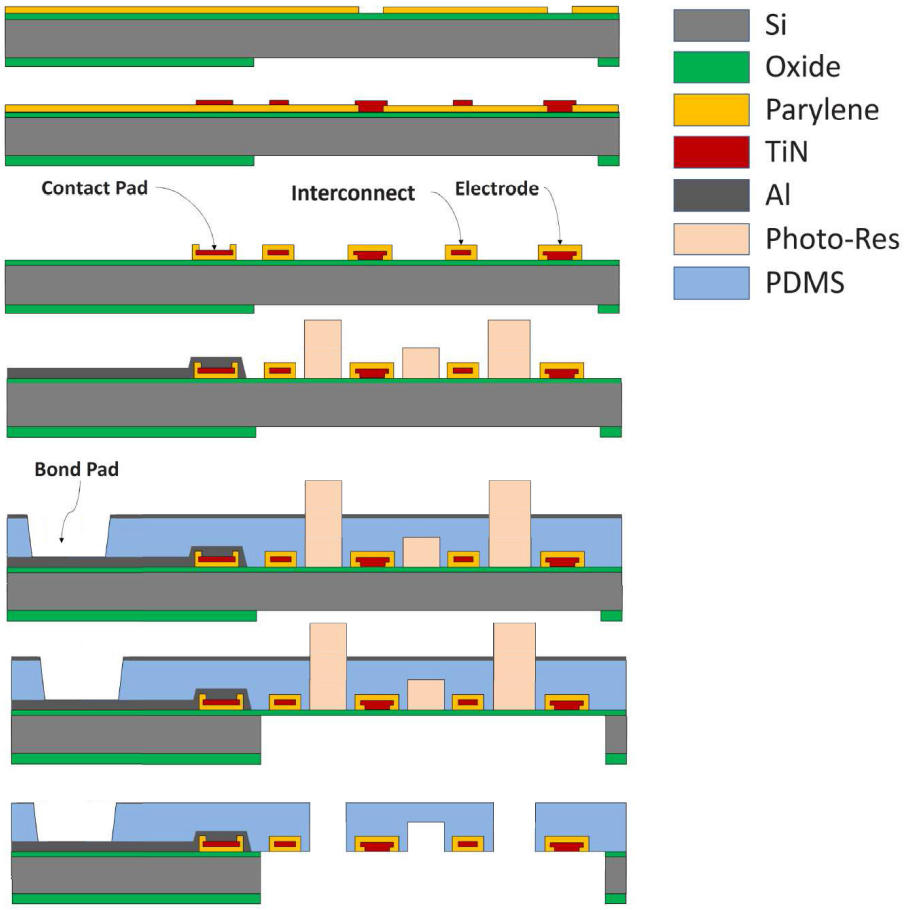

Figure 3.5: Selective deposition of PDMS to fabricate holes. One extra mask steps is required. *Drawing adapted from [45].*

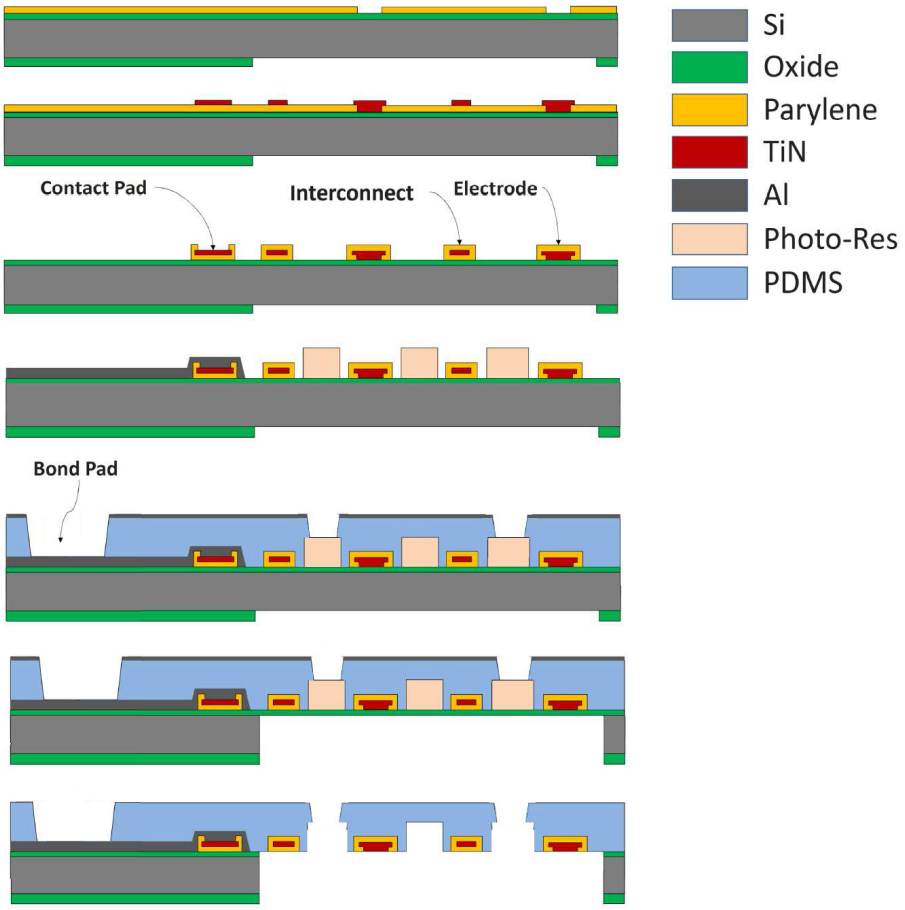

Figure 3.6: Selective deposition and selective removal of PDMS to fabricate holes. No extra mask steps are required. *Drawing adapted from [45].*

Chapter 4

Properties and processing of PDMS

Polydimethylsiloxane (PDMS) is an important material in the fields of microfluidics, Lab-on-Chip and Organ-on-Chip, as it is easy to fabricate relatively complex microfluidic structures using molding techniques, without the need for advanced tools or facilities. However, PDMS is difficult to work with in a microfabrication cleanroom environment. The realization of small feature sizes, or achieving high reproducibility and mass production is therfor challenging. Certain properties of PDMS, such as biocompatibility, stretchability, flexibility, optical clearness and chemical stability, make it worthwhile to investigate whether PDMS is processable with standard microfabrication cleanroom tools. Although some techniques, such as etching, have been proposed in literature, most of these techniques are still suboptimal. As a result, the use of PDMS has not yet gone from an experimental to a mature stage. Basic problems like slow etch rates, poor adhesion to many materials and stress issues make for example even depositing a photoresist layer on PDMS problematic.

In this Chapter the properties of PDMS are reviewed and current techniques to process PDMS are evaluated. In the last Section new techniques are introduced that were developed in the course of this project.

4.1 Properties of PDMS

The properties of PDMS and modifications of these properties have been excellently described by previous members of this group [7] and in literature [37, 39], but those that are relevant to explain results obtained in the next Sections will be described briefly. The PDMS used in this research was Dow Corning Sylgard®.

PDMS is the most frequently used silicone. The backbone of silicones is an alternating chain of silicon and oxygen atoms, leaving two free bonds

on the silicon atom. In PDMS, these bonds are both filled with a methyl group (Fig. 4.1). Like most polymers, the chain is typically long and it is available in many different viscosities. For Cytostretch the elastomer (i.e. elastic polymer) is used: silicon rubber. Silicon rubber provides good elasticity without causing permanent deformation.

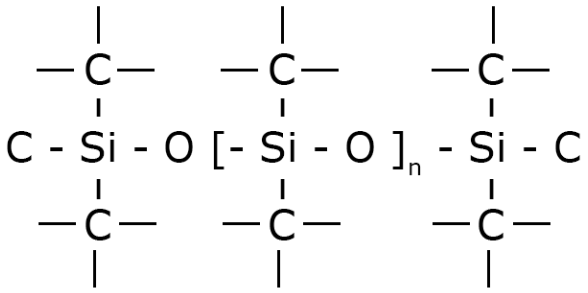

Figure 4.1: Molecular formula of polydimethylsiloxane.

The molecular configuration of PDMS makes it highly hydrophobic, resulting in a water contact angle of 110 °. This hydrophobic property is a downside when for example depositing photoresist. The surface is highly non-polar, which is why the photoresist does not spread out when it comes in contact with the PDMS. This problem can be easily overcome by subjecting PDMS to a short oxygen plasma [4, 29], which reacts with the methyl groups to form CO or CO_2 and H_2O, leaving SiOH-groups (silanol) at the surface of the PDMS.

The PDMS used in this research exists of two parts: an elastomer and a curing agent, that are mixed 10 to 1, respectively. Curing can be done at room temperature, but the process can be accelerated by using temperatures of up to 200 °C [17]. Deposition of PDMS on a silicon wafer is done with a manual spin coater and is done directly after mixing and degassing. The spin speed, mixing ratio, curing temperature and curing time all influence the Young's modulus of PDMS [1, 21, 24, 36]. The average film thickness used in this work is 11 μm, which is the smallest thickness achievable while limited by a maximum spin speed of 5500 RPM, without diluting PDMS.

4.2 Deposition of materials on PDMS

One of the problems encountered when using PDMS as a material in a cleanroom process flow is the adhesion of PDMS on other materials and

deposition of other materials on PDMS. When materials are deposited on PDMS, three issues arise: (i) poor adhesion to the deposited material, (ii) a low maximum allowed temperature budget during deposition and (iii) stress induced during the deposition of the material at elevated temperatures.

4.2.1 Adhesion

Bonding other materials to fully cured PDMS is typically done by oxidizing the PDMS surface by means of an oxygen plasma to form SiOH-groups. These groups can make covalent bonds with other OH-groups, such as PDMS itself, silicon dioxide or oxidized glass, resulting in a Si-O-Si bonding and the release of a water molecule (H_2O) [4, 29, 40]. The more hydrophilic the surfaces are, the stronger the bond they form. It has been investigated previously, that the same holds for bonding of uncured PDMS to a PDMS substrate [7].

4.2.2 Deposition temperature

The temperatures over which PDMS remains chemically stable, ranges from -45 °C up to 200 °C [17]. In cleanroom processes this is considered to be a very low temperature range, since many processes take place at 350 °C or higher. Being limited to this temperature range makes many process steps impossible. Deposition of silicon dioxide, even with the relative low-temperature PECVD process, is not possible when PDMS is present. PDMS will 'burn' when exposed to a temperature higher than 200 °C (Fig. 4.2).

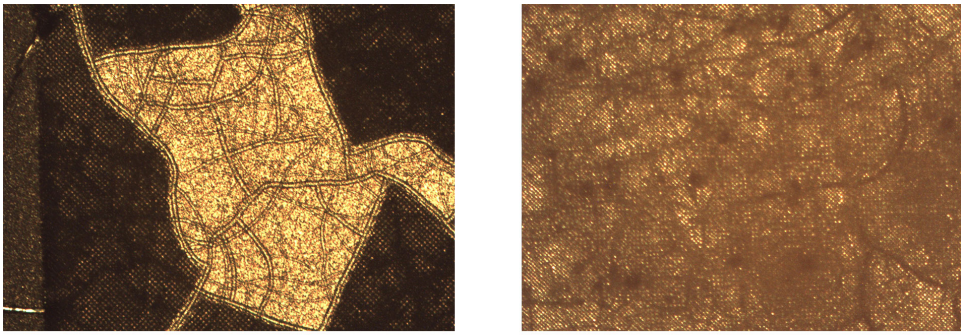

Figure 4.2: Two pictures of aluminum deposited on PDMS at a too high temperature.

For certain processes high temperatures are essential for deposition, but for others - such as metal deposition - the temperature is high because the process heats up the substrate through. In such case it is possible include 'wait steps' to give the substrate time to cool down before continuing the process. Typically, low-temperature processes with cooling steps produce

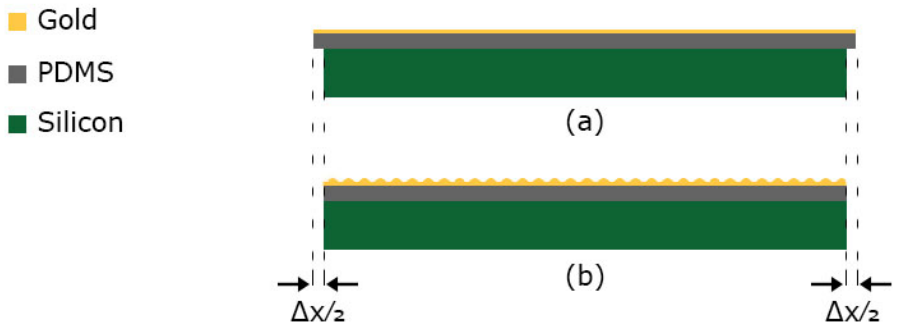

Figure 4.3: Schematic of thermally induced stress in a gold layer after deposition on PDMS. The gold is deposited on an thermally expanded PDMS substrate (a), which is ΔX times larger then at room temperature. When the substrate cools down, the gold surface has to decrease a similar amount although the material itself only shrinks by $\Delta/20$. This stress results in wrinkles on the gold surface.

layers that are of lower quality. For metals, this means a decrease in electrical conductivity of the resulting layer.

4.2.3 Thermally induced stress

In the previous Section, the limitations of PDMS with respect of the range of temperature were described, but the thermal expansion of PDMS introduces another temperature related limitation. The coefficient of thermal expansion (CTE) of PDMS is quite high ($\alpha_L = 300 \times 10^{-6}$ / °K) [10] compared to that of many other materials, such as gold. When PDMS is heated up during the deposition of such a material, PDMS expands. Since the CTE of a thin gold film is more than 20 times lower ($\alpha_L = 9.6$ to 13.6×10^{-6} / °K) [38], the shrinkage of the PDMS during cooling is 20 times more than that of gold, resulting in wrinkles in the deposited gold layer (Fig. 4.3).

The CTE of photoresist ($\alpha_L = 30 \times 10^{-6}$ / °K) [42, 48] differs from PDMS. The mismatch between expansion coefficients becomes problematic when thick layers of photoresist are used [43]. Instead of forming wrinkles, it results in long cracks in the photoresist. An explanation for this is that there is too much material to bulge into wrinkles, so the material breaks to cope with the stress.

Cracking of photoresist is a problem if the resist is used as mask for etching. The cracks are etched into the layer underneath, resulting in unwanted patterning, often over a large area of the wafer, producing a die yield of zero (Fig. 4.4). To overcome this problem the transition from hot to cold should be slow [43], to distribute the stress slowly into the layer. Unfortunately, this takes quite some time and the best results are achieved by heating up

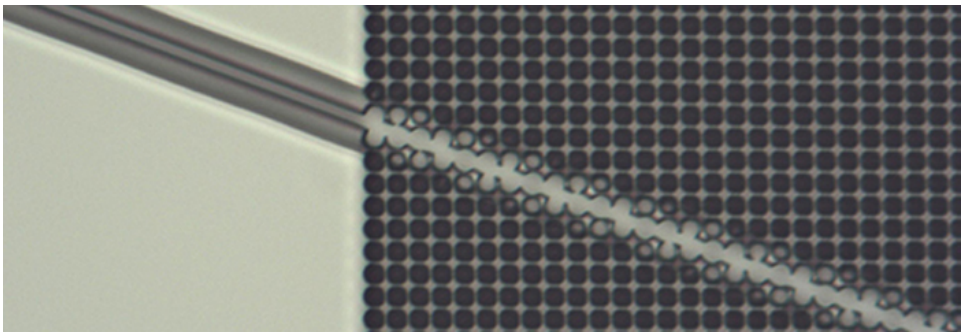

Figure 4.4: Thermally induced crack in the photoresist that has been etched into the PDMS membrane.

a cooling plate instead of letting a hotplate cool down [7]. However, this is not a standard process, it is time consuming and is unsuitable for mass production.

4.3 Selective deposition of PDMS

There are two techniques to selectively deposit PDMS, both based on the fact that PDMS is ultimately well suitable for casting. Two properties in particular are contributing to the success of these techniques: (i) no bonding to the master or mold and (ii) replication of a wide range of feature sizes. The use of molds in microfabrication is reviewed in Section 4.3.1, and Section 4.3.2 discusses an alternative approach, based on the same advantageous properties, but more cleanroom compatible: spin casting.

4.3.1 Molding

Molding is the technique of choice for many biomedical laboratories since it does not require expensive machines to cast an existing master. The master can be fabricated elsewhere, and can be used an infinite number of times. Low tech and low cost methods are also available for rapid prototyping, changing the master to any desired feature within a certain range of feature sizes [20, 34]. Molding is also possible within the microfabrication cleanroom. A mold can be pressed into a wafer with a layer of uncured PDMS to act as a master for the PDMS. This technique is used by Huh et al. [33] to fabricate membranes with holes, but their approach introduces certain issues and limitations. First of all, the process is manual and time consuming since the wafer and mold need to be cured at room temperature for 24 hours. Secondly, there is a lower limit to the thickness of the membrane, since these membranes need to be handled with tweezers after they are removed from

the wafer, in order to incorporate the membranes in a device.

4.3.2 Spin casting

Another method for selective deposition of PDMS is blocking certain parts of the substrate for PDMS using photoresist [7] (Fig. 4.5). Good results have been achieved with this technique, but two issues need to be addressed. First of all, the resist structures after spin casting are nearly always covered with a thin layer of PDMS, which needs to be removed by reactive ion etching (RIE). Unfortunately, the photoresist that is used as a cast can get highly cross linked, since PDMS is transparent to ultraviolet light [13, 47]. Removing this mold is therefor not possible by just dissolving it in acetone, but the process requires an oxygen plasma which attacks the surface of the PDMS and is able to crack it. If the etching of the thin layer of PDMS is done using wet etching of PDMS (see Section 4.4), this problem will not occur.

The second issue is the formation of high aspect ratio features in photoresist. Since the PDMS layer in the Cytostretch device is quite thick (10 to 20 μm), the photoresist structures should be preferably higher than the PDMS layer (i.e. > 20 μm). Consequently, the small features required for the holes in the PDMS membrane require high aspect ratio resist pillars. Although it is possible to fabricate high aspect ratio's by using for example AZ9260 or SU8 [12], both resins introduce difficulties. AZ9260 has quite a high risk of collapsing when a thick layer of a heavy polymer is spun on [51]. SU8 is stronger, but hard to remove without residues [19]. In previous studies, spin casting was used to achieve bond pad and electrode openings with a minimum diameter of 25 μm [7]. For the small holes needed in membrane of the Cytostretch Skin device, this technique has not been applied yet.

4.4 Selectively removing PDMS

The previous Section discussed the selective deposition of PDMS, but the inverse is also possible: selective removal. Etching is amongst the most important processes in microfabrication, but at the same time it is one of the bottlenecks of PDMS processing. Many attempts have been made to develop etching processes, but slow etch rates, tapered sidewalls and etching residues are issues yet to overcome. In this Section current state of the art techniques to etch PDMS will be reviewed, before exploring new techniques in Section 4.5.

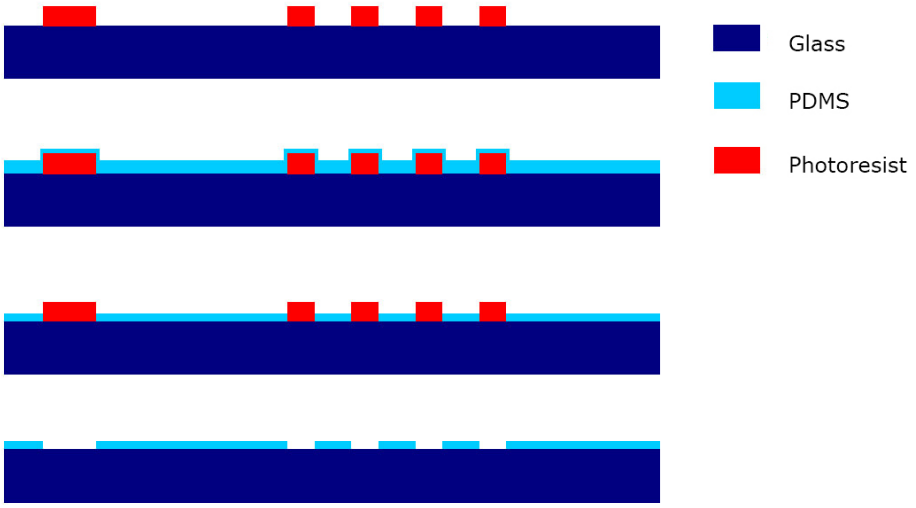

Figure 4.5: Process flow of patterning PDMS by spin casting [7].

4.4.1 Dry etching using CF_4 and O_2

Most polymers are etched in an oxygen plasma, but PDMS, which is silicon based, is not. The preferred dry etching method for PDMS is based on a fluoride chemistry, similar to the etching chemistry used for silicon. Optimizing this chemistry, Garra et al. found that a 1:3 mixture of O_2 and CF_4 resulted in an optimum etch rate of 0.33 μm/min [25]. The etching was quite anisotropic, with a lateral etching of 12.5 μm per side at a depth of 80 μm or an anisotropic etching ratio of 6:1 between vertical and lateral direction. The sidewall angle has not been measured, but it can be calculated as $\alpha = \arctan 6/1 = 80\,^\circ$. As clearly shown by Fig. 4.6, the surface roughness is high; about 10 μm peak-to-peak, at least partly caused by non-volatile by-products of the plasma. Cleaning with a water jet to remove the by-products might decrease the surface roughness. Without improving the surface roughness, the minimum feature size for etched PDMS will be limited by the lack of a homogeneous step height. In [25] it is shown that the minimum depth is limited by the surface roughness to is 50 μm, resulting in a lateral under etch of $50/6 = 8.3$ μm per sidewall. The minimum line width will thus be approximately $8.3 * 2 = 16.6$ μm. The minimum feature size will also depend on the location of the feature on the wafer, since plasma etchers are bound to a have a non-uniform etch rate across the center and the edge of the wafer. The selectivity towards the hard etch mask material (aluminum) is quite good, but it is possible that back-sputtering occurs due to the ion bombardment, causing micro masking at undesired locations. The

latter might explain the high surface roughness, as indicated before [25]. For this reason, aluminum is not an ideal hard etch mask material.

The figures of merit for the dry etching method are summarized in Table 4.1.

Figure of merit	quantitative data	qualitative data
Anisotropic etching	6:1	+
Etch rate	0.33μm	−−
Sidewall angle	80 °	++
Minimum feature size	16.6μm	−−
Surface roughness (peak-peak)	10μm	−−
Etch rate of masking material	NA (Al)	+
Etch rate uniformity	NA	−

Table 4.1: Figures of merit for PDMS dry etching using CF_4 and O_2 [25].

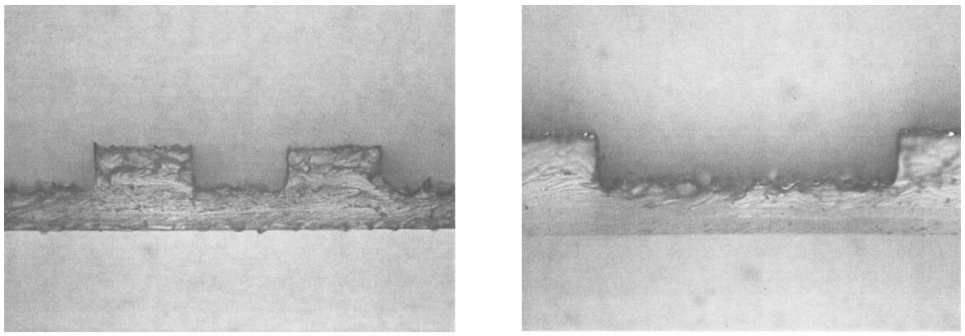

Figure 4.6: Cross sections of two different structures, (a) and (b), etched in PDMS as seen under the optical microscope at 20x magnification. The twin structures in (a) are roughly 140 μm wide and 60 μm high. The rectangular etch cavity in (b) is 350 μm wide and 60 μm deep. The measurement reticle is not visible in the pictures. *Image and caption cited from [25].*

Another fluoride chemistry which has been proposed is a plasma consisting of only SF_6 with a reported etch rate of 0,8 μm/min [57]. Although this etch rate is higher than the etch rate of CF_4 and O_2 mixture, the surface roughness is claimed to grow linear with 0.4 μm/min, which means that 50% of the etch rate can be discarded. Additionally, no etch rates are shown for longer etch times and since those etch rates are likely to drop when etching deeper in the surface, the average etch rate is believed to drop as well. Furthermore, no data about isotropy or sidewall angles are available. For these reasons, most research groups prefer CF_4 and O_2 chemistry.

In our group it was found that a combination of SF_6 and CF_4 gave an etch rate of 0.45 μm/min, but a large number of remnants was found [52].

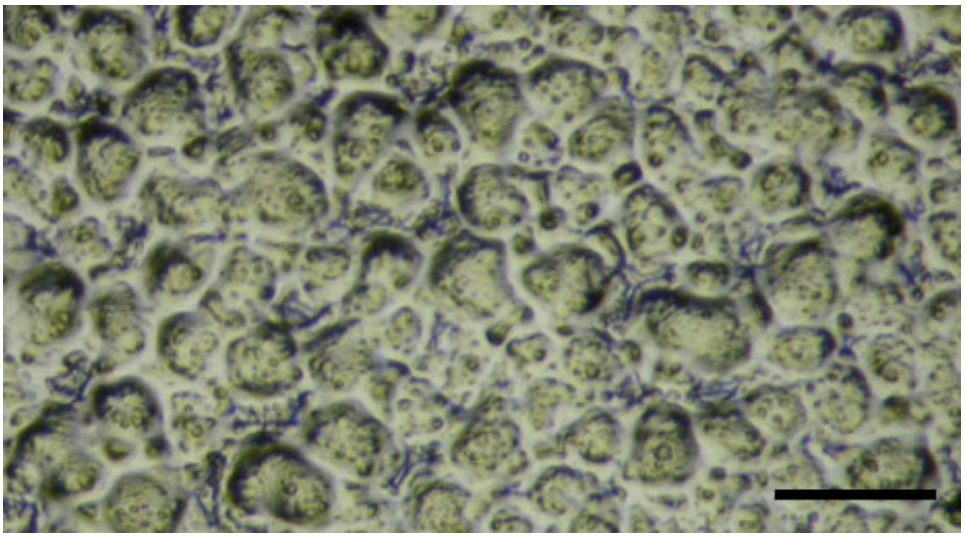

Figure 4.7: Light microscopy pictures of a PDMS film after 8 minutes wet etching. The measurement bar indicates 100 μm. *Image cited from [3].*

No literature was found on the usage of other chemistry than fluorine for dry-etching PDMS.

4.4.2 Wet etching using NMP and TBAF

A faster method to etch PDMS is wet etching. This is being done using a solution of *N*-methyl pyrrolidinone (NMP) and tetra-butyl ammonium fluoride (TBAF) in a ratio of 3:1, respectively [3]. This solution is also based on fluoride chemistry to etch the silicon backbone of PDMS and etches with an etch rate of 1.5 μm/min. The etching is completely isotropic, so no etching difference is found in the lateral direction, when compared to the vertical direction, resulting in a circular shaped sidewall with an angle between 0 ° at the top corners and increasing up to 90 ° near the bottom of the layer, describing one quarter of a circle with a radius equal to the etch depth. This limits the minimum feature size to features with a width equal to the etch depth. The surface roughness is better compared to dry etching, but still there is a peak-to-peak height of 0.7 μm (Fig. 4.7). Although the etch rate is uniform over the wafer, due to the homogeneous concentration of NMP and TBAF throughout the etching solution, the etch bath has to be refreshed every 10-15 minutes to ensure a constant etch rate. After this time the etch rate will drop because the solution becomes saturated. Finally, the selectivity towards the masking material (aluminum) is very good, and the etch rate of aluminum can considered to be zero.

The merits of this wet etching method are summarized in Table 4.2.

Figure of merit	quantitative data	qualitative data
Anisotropic etching	1:1	--
Etch rate	1.5μm/min	++
Sidewall angle	[0 °,90 °]	--
Minimum feature size	∼depth	--
Surface roughness (peak-peak)	0.7 μm	-
Etch rate of masking material	0 μm/min (Al)	++
etch rate uniformity	1:1	++

Table 4.2: Figures of merit for PDMS wet etching using 3:1 NMP/TBAF [3, 25].

The main disadvantages of wet etching are (i) a lack of anisotropic etching behavior, making it unsuitable for small feature sizes, and (ii) the solution has to be refreshed several times and NMP is a reprotoxic solvent, to be handled with great care.

4.4.3 Lasering ablation

Removing material by means of laser ablation is a less standardized process, but it is sometimes used in microfabrication because of its speed, accuracy and ability to remove almost any material [55]. The laser burns holes in the substrate and the feature size is determined by the minimum spot size which in turn is determined by wavelength of the laser. At this point, there is no laser available that is capable of making holes smaller then 25 μm at our facilities, and tests with thin films have not been done yet, but good results were achieved during tests using quite thick PDMS membranes (Fig. 4.8). Besides the relative large minimum feature size, another disadvantage is the fact that this technique is not standard for batch processable microfabrication. Also, the surface around the holes is quite rough, most likely due to heating of PDMS.

4.5 New techniques

As mentioned before, developing new techniques for the processing of PDMS in the microfabrication cleanroom environment is important for mass production of Organ-on-Chip models. Three new techniques have been investigated during this research, two of which are used in the final fabrication of the device. The next Sections explain techniques to improve the deposition on PDMS, a new way to selectively deposit PDMS, as well as a new, faster etching chemistry, respectively.

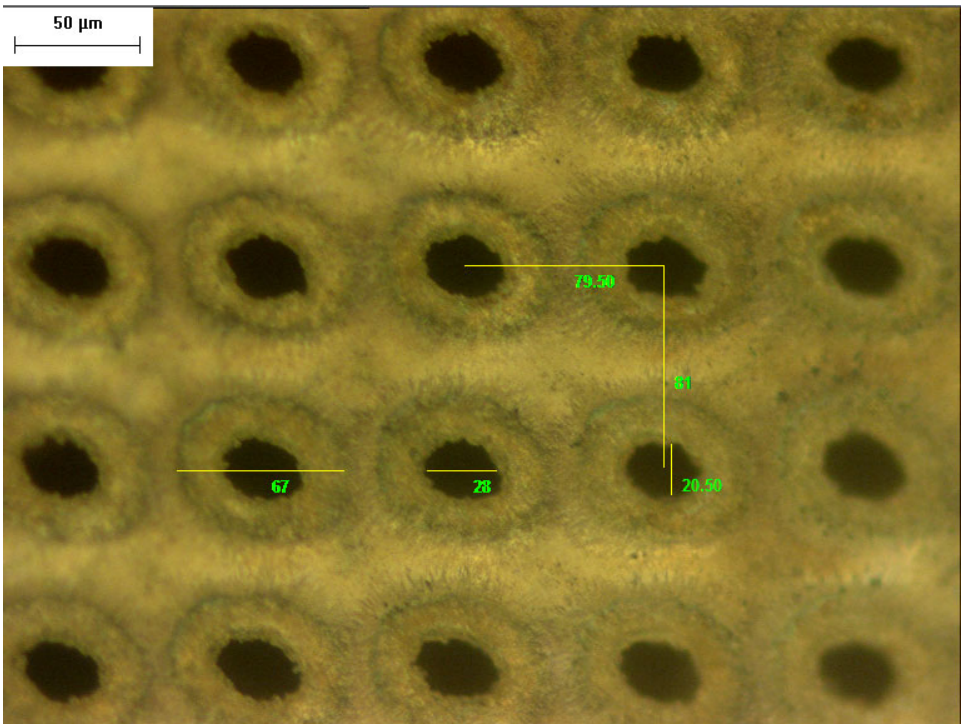

Figure 4.8: Light microscopy pictures of PDMS holes cut by a laser.

4.5.1 Photoresist spin coating

As mentioned in the first section of this Chapter, thermally induced stress is a problem in the deposition of materials on PDMS. During this research, a new technique was developed to overcome this problem by the deposition of a stress buffer in the form of an intermediate layer that can cope with the stress induced by thermal expansion of PDMS. The technique has been demonstrated for the deposition of a thick photoresist layer (AZ9260), in which cracks will normally form as a result of rapid changes in the temperature of the substrate. Before spin coating the photoresist, a 250 nm thin layer of aluminum (with 1% silicon) is sputter coated on top of the PDMS at room temperature. This aluminum layer limits the expansion of PDMS while the photoresist is softbaked (Fig. 4.9). Since the CTE of aluminum ($\alpha_L = 22 \times 10^{-6}$ / °K) is almost equal to the CTE of photoresist, no significant stress is introduced in the thick masking layer.

4.5.2 Microporous PDMS

A novel way to develop microporous PDMS was proposed by Choi et al. [15]. Choi describes a method to make sponges of PDMS using sugar cubes as

Figure 4.9: Close-up of a thin aluminum layer as stress buffer between PDMS and photoresist. It is assumed that the thermal expansion of aluminum and photoresist is zero, in order to emphasize the mechanism.

casting material. Since sugar readily dissolves in water, it is quite simple to remove the cast. What is particularly interesting, is the sugar cube is placed in a thin layer of PDMS and due to the capillary effect, the polymer fills the small empty spaces withing the cube. The experiments were repeated and good results were obtained (Fig. 4.10). Such a structure could provide the holes needed in the membrane for the Cytostretch Skin model if the holes could be made smaller by casting a mold of smaller sugar crystals. It was attempted to coat a wafer with a layer of sugar crystals, but it melted too fast and it caramelized, rendering the wafer useless. Additionally, experiments have been conducted with starch-based polymers, which are also highly soluble in water. Although the results were promising and similar to the results obtained from the sugar mold, no manageable way has been found to apply such a polymer on a wafer while influencing the hole size.

Concluding, an effortless way to apply this technique on wafer scale has yet to be found.

4.5.3 Dry etching using SF_6 and Cl_2

Due to its silicon backbone, PDMS has only been etched using fluoride chemistry. A chlorine chemistry, as used for example for dry etching aluminum, has so far not been considered. Accidentally, it was discovered during this project that a standard recipe to etch aluminum (a gas concentration of 30 standard cubic centimeters per minute (sccm) Cl_2 and 40 sccm HBr, a pressure of 5 mTorr and RF platen power of 50 Watt) etches PDMS almost twice as fast as a standard fluorine chemistry (Fig. 4.11). The sidewall angle of the etched features were not measured, but the sidewalls were less steep when compared to fluoride etching and were estimated to be around 60 °.

Figure 4.10: Microporous PDMS 'sponge' fabricated as described by [15].

Although some surface roughness is present, it was significantly less, when compared to fluoride etching (Fig. 4.12).

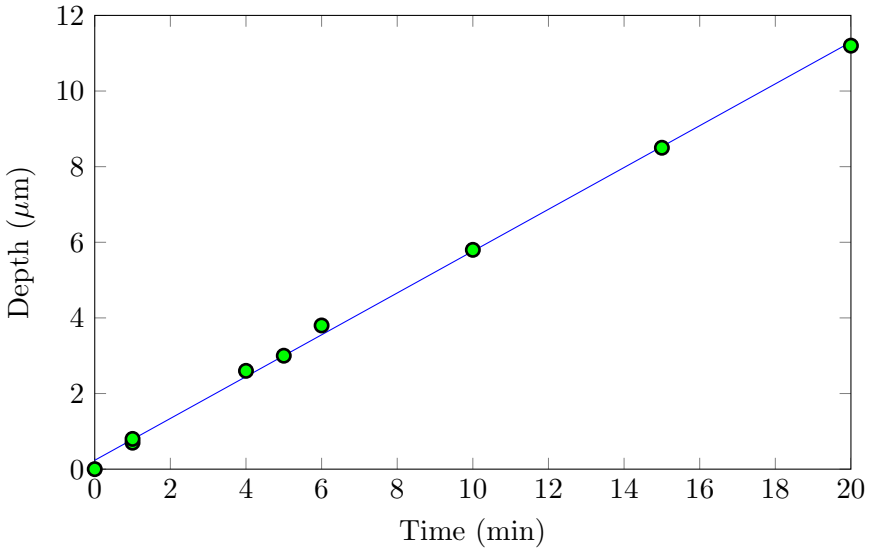

Figure 4.11: Etch depth versus time at a gas mixture of 30 sccm Cl_2 and 40 sccm HBr. The blue line is a first order polynomial fitted line and has a slope of 0.55 μm/min.

Investigating the influence of the platen power on the etch rate was done by keeping the gas mixture constant and introducing a variation to the platen power. Figure 4.14 shows that the etch rate of the PDMS did not increase above a platen power of 50 watts, but the etch rate of the masking layer of photoresist did increase. For this reason, the platen power was set to 50 watt. In order to investigate the active chemistry in the plasma,

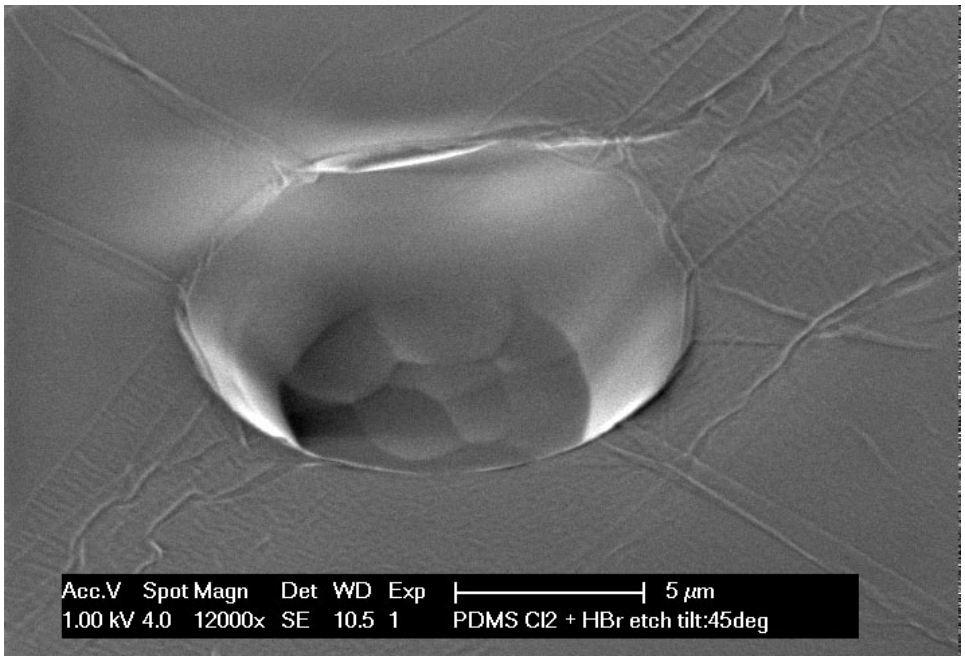

Figure 4.12: SEM microphotograph of a dry etched hole in PDMS using Cl_2 and HBr chemistry.

experiments were done varying the values of the flow of Cl_2 and HBr. The results indicate that chlorine was the active component in the plasma, since the etch rate dropped without the presence of chlorine, while the addition of HBr did not result in a difference in etch rate (Fig. 4.14).

To optimize the etching process, while maintaining the low surface roughness, increasing the anisotropy, and increasing the etch rate even further, a combination of fluoride and chloride chemistry was tested. Varying the ratio of the gas mixture of SF_6 and Cl_2, the highest etch rate was found to be 1.5 μm/min. Although differences of just a few 100 nm were found, the highest etch rate is achieved with a gas ratio of 30 sccm Cl_2 and 10 or 20 sccm SF_6 (Fig. 4.15). For the gas ratio of 30:10 sccm, the etch rate was constant up to at least 15 μm (Fig. 4.16) and it is assumed that the gas ratio of 30:20 gives a similar result. The masking material used was photoresist (AZ9260), towards which the plasma had a poor selectivity of almost 1:1. The etching is very anisotropic and the angle of the sidewall is estimated to be greater than 85 ° (Fig. 4.18). The surface roughness of the sidewall is clearly visible and does not exceed more than several dozens of nanometers. The minimum feature size is no longer limited by the surface roughness and is significantly reduced. The etch rate uniformity is comparable to the previously described dry etching method. Exact measurements have not been done, but as can be seen in Fig 4.19, some holes on the edge of the wafer are not etched at

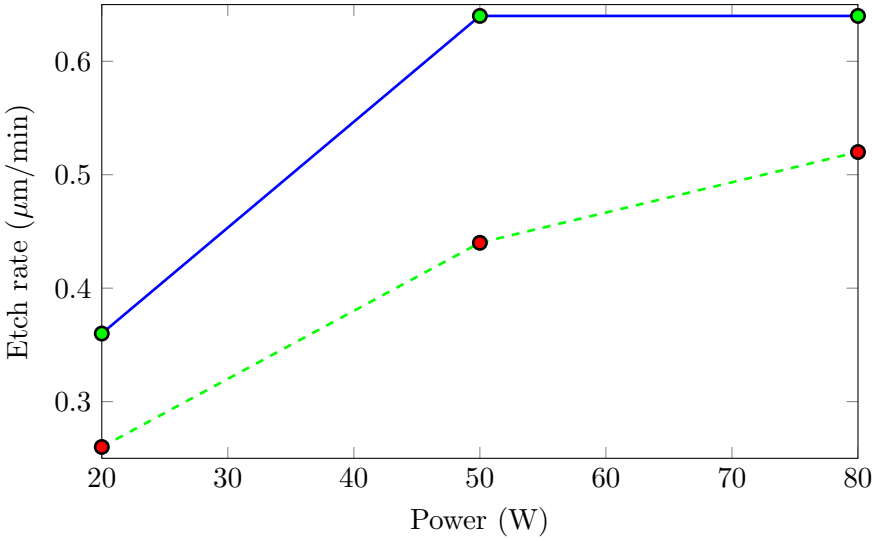

Figure 4.13: Etch rate of PDMS (green measurement points) and photoresist (red measurement points) at different RF platen power for a gas mixture of 30 sccm Cl_2 and 40 sccm HBr.

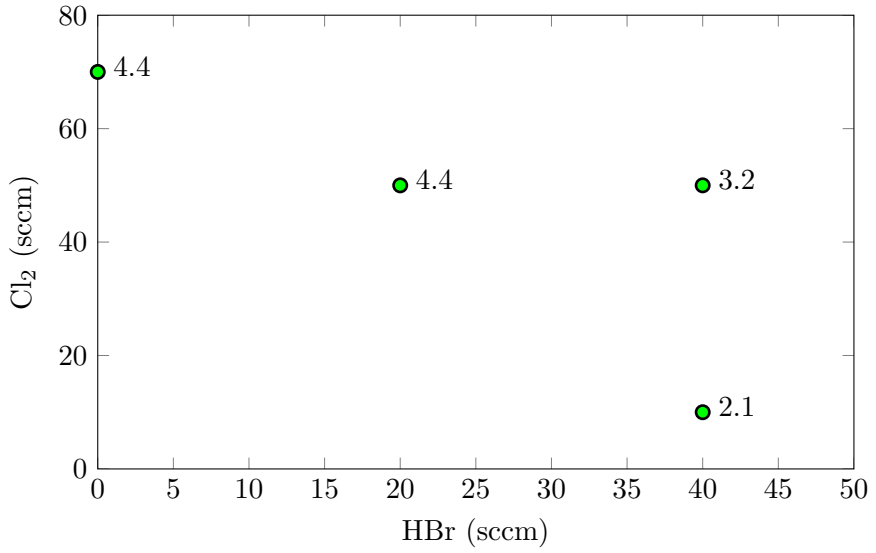

Figure 4.14: Etch depths after etching for 5 minutes with different mixtures of Cl_2 and HBr.

Figure of merit	quantitative data	qualitative data
Anisotropic etching	>6:1	++
Etch rate	1.5 μm/min	++
Sidewall angle	>85 °	++
Minimum feature size	<2∗(depth/tan 85 °)	++
Surface roughness (peak-peak)	<300μm	+
Etch rate of masking material	1.25 μm/min (PR)	−−
etch rate uniformity	NA	−−

Table 4.3: Figures of merit for PDMS wet etching using using SF_6 and Cl_2.

all. Over a width of 10 mm the etch result dropped from completely etched (11 μm deep) to not etched at all.

The figures of merit for this new etching method are summarized in Table 4.3.

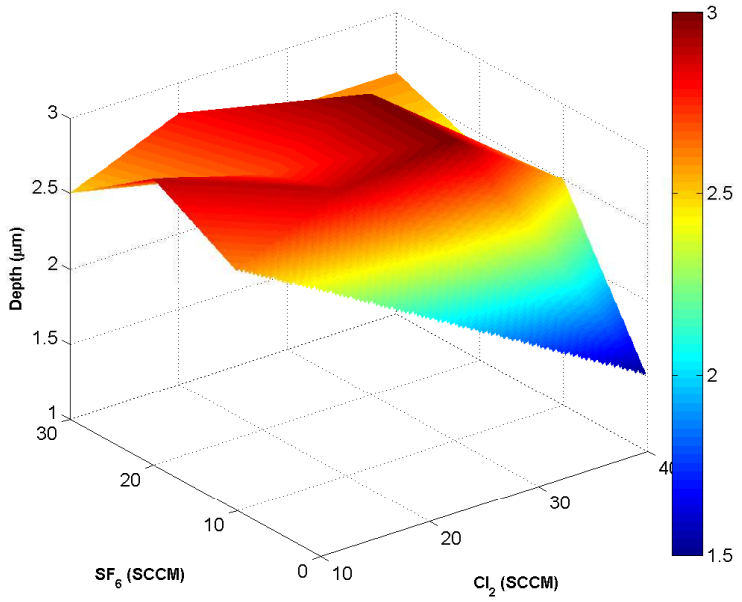

Figure 4.15: Etch depth after 2 minutes with different sccm mixtures of Cl_2 and SF_6.

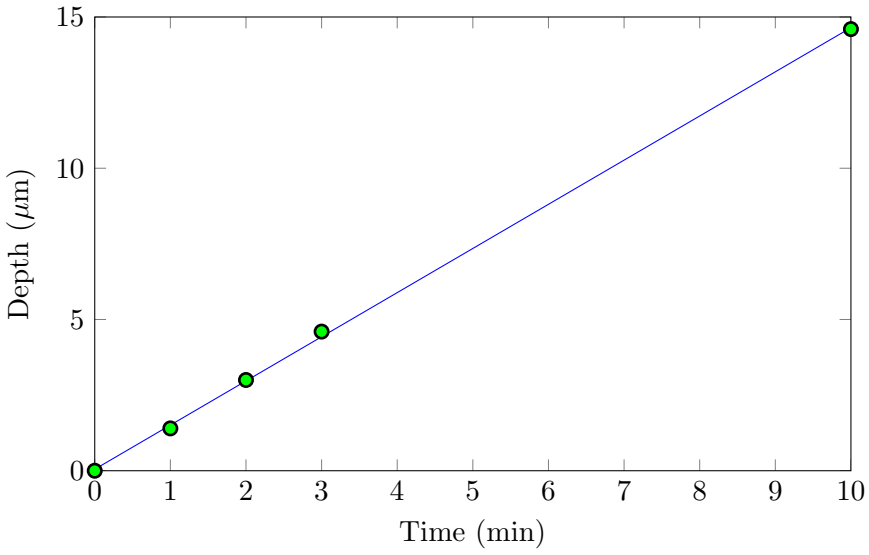

Figure 4.16: Etch depth versus time with a mixture of 30 sccm Cl_2 and 10 sccm HBr. The blue line is a first order polynomial fitted line and has a slope of 1.46 μm/min.

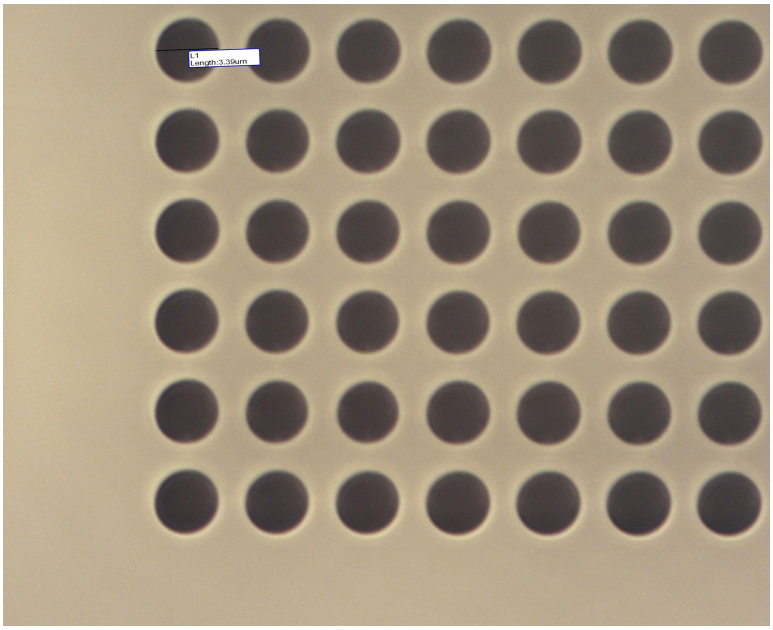

Figure 4.17: Image of dry etched PDMS structures using Cl_2 and SF_6. The size of the holes is 3.4 μm.

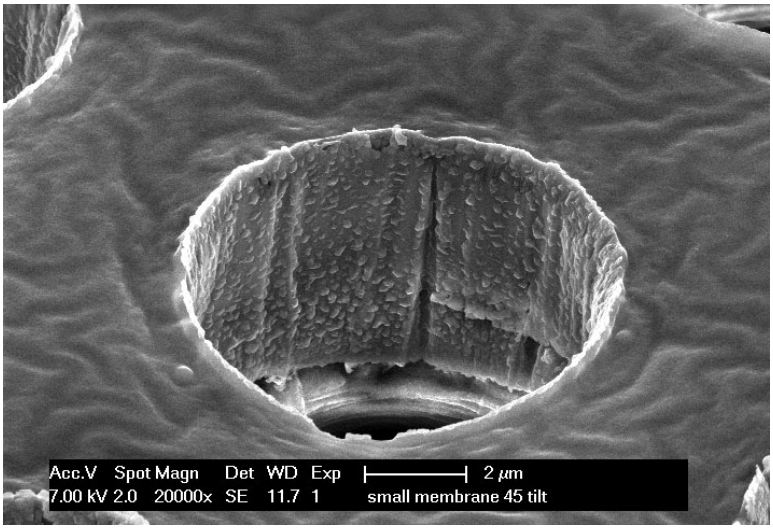

Figure 4.18: SEM from a dry etched PDMS structure using Cl_2 and SF_6.

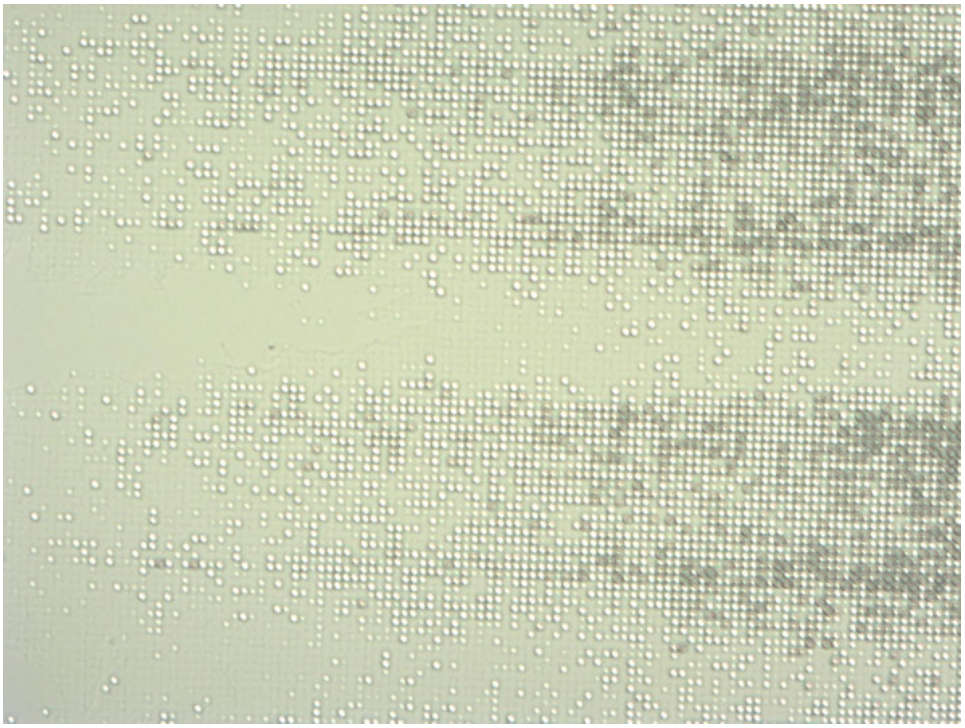

Figure 4.19: PDMS structures located on the edge of the wafer, dry etched using Cl_2 and SF_6.

Chapter 5

Fabrication

In Chapter 3, three process flows have been proposed to fabricate the Cytostretch Skin device, based on selective removal of polydimethylsiloxane (PDMS), selective deposition of PDMS and a combination of both. In this Chapter experiments are done to fabricate the Cytostretch Skin device according to the different proposed process flows using the processing techniques described in Chapter 4. For the sake of convenience the design requirements are repeated here:

- a perforated membrane with a hole diameter in the range of 5 to 8 μm;
- a membrane diameter of at least 10 mm;
- cell plating possible on both sides of the membrane.

Before fabrication of the holes and the complete development of the device is discussed, the designed mask layout is discussed in the first Section.

5.1 Mask design

In order to meet the design requirements of the Cytostretch Skin device, new masks were designed. In the first mask design, the membrane was rectangular (15 x 15 mm^2) to maximize the area for cell culturing (Fig. 5.1). The hole size within the membrane varied between different membranes and had a diameter of either 2 μm with a minimum spacing (center to center) of $\sqrt{5^2 + 5^2} = 7.07$ μm and a maximum spacing of 10 μm (Fig. 5.2), or a diameter of 5 μm with a minimum spacing of $\sqrt{7^2 + 7^2} = 9.90$ μm and a maximum spacing of 14 μm (Fig. 5.3). The spacing was minimized in order to increase the migration possibilities of the Langerhans cells through the membrane.

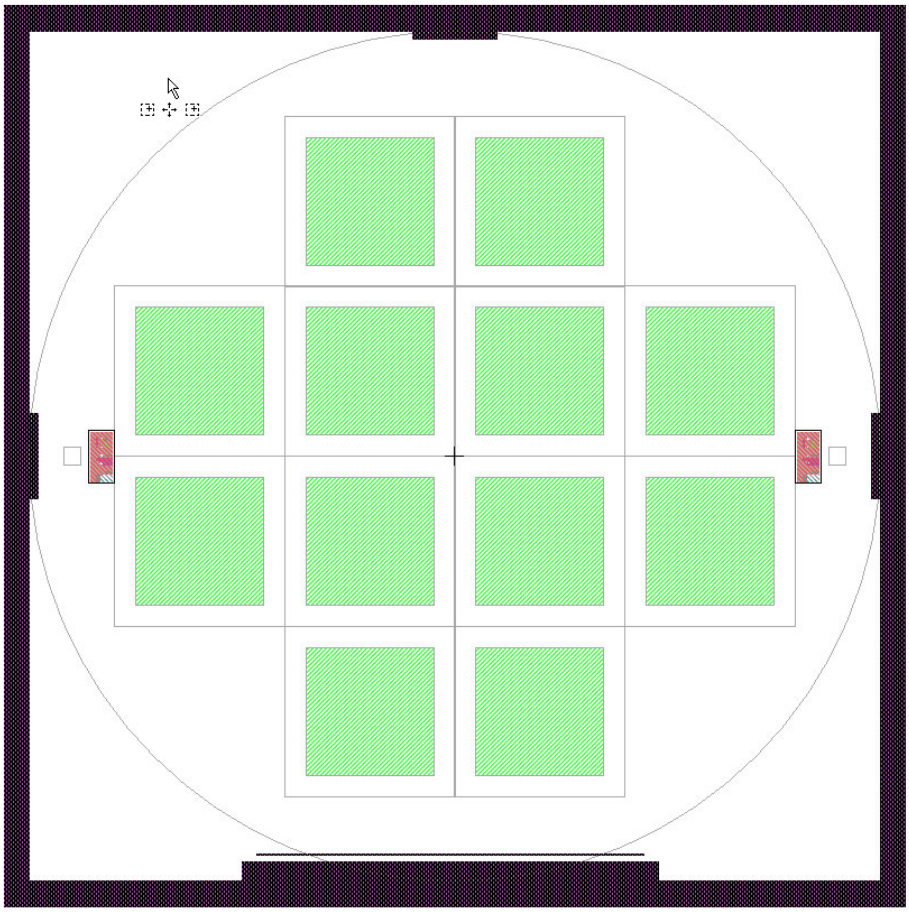

Figure 5.1: Screenshot of the first version mask design (BACK) for the Cytostretch Skin device. The green squares indicate the membrane size (15 x 15 mm^2).

The inverted mask design of the holes was developed in order to make photoresist pillars instead of holes using positive photoresist.

During fabrication, two major flaws in the mask design became apparent. Firstly, etching the PDMS - even with the most anisotropic technique - did not result in a pattern of holes, but in a pattern of 'hills'. Figure 5.4 shows that the spacing between the holes was not sufficient and the separation between the individual holes was lost. This could be the result of isotropic etching, but since the results as depicted in the previous Chapter show steep side walls, this is not likely. It is more likely that it originates from the limits of the patterned photoresist masking layer, in which too thin parts of the photoresist might have collapsed.

The second problem encountered was that the rectangular membrane broke when it was released (Fig. 5.5), most likely due to the built up stress

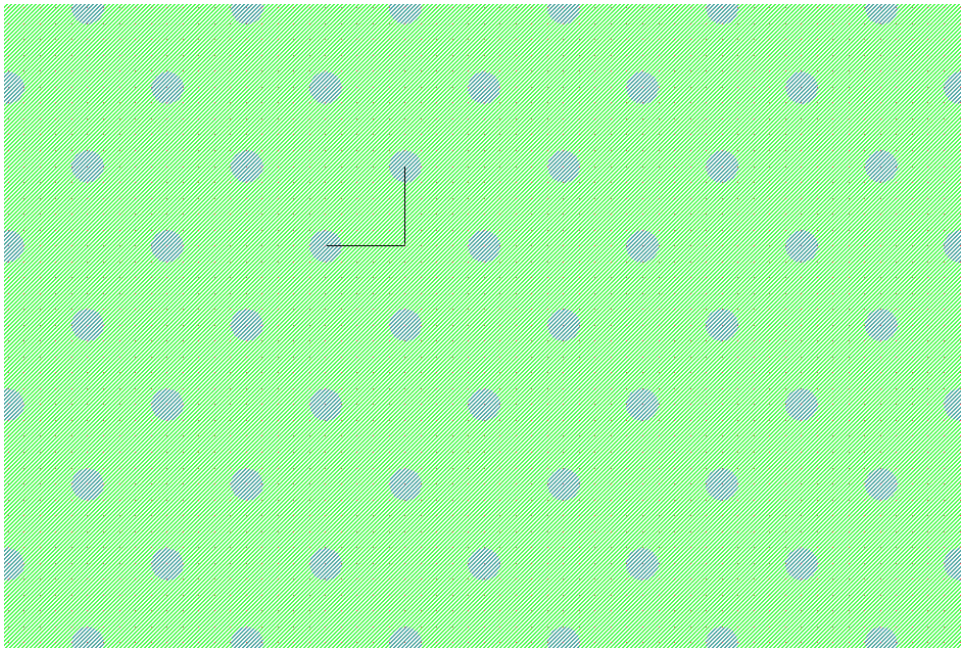

Figure 5.2: Closeup of the first version of the 2 μm hole pattern (HOLES). The black measurement bars indicate 5 μm.

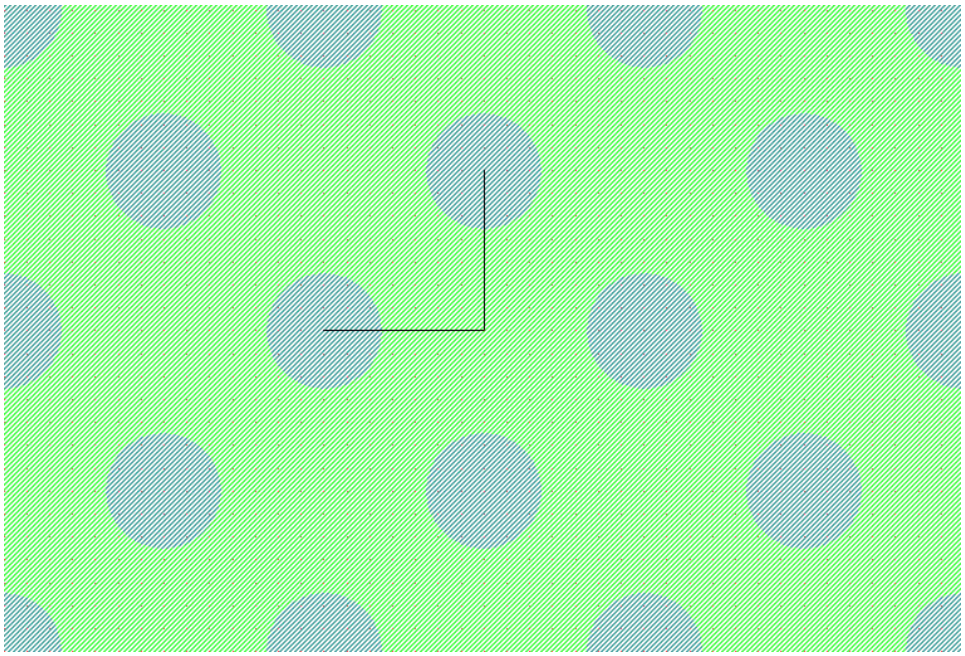

Figure 5.3: Closeup of the first version of the 5 μm hole pattern (HOLES). The black measurement bars indicate 7 μm.

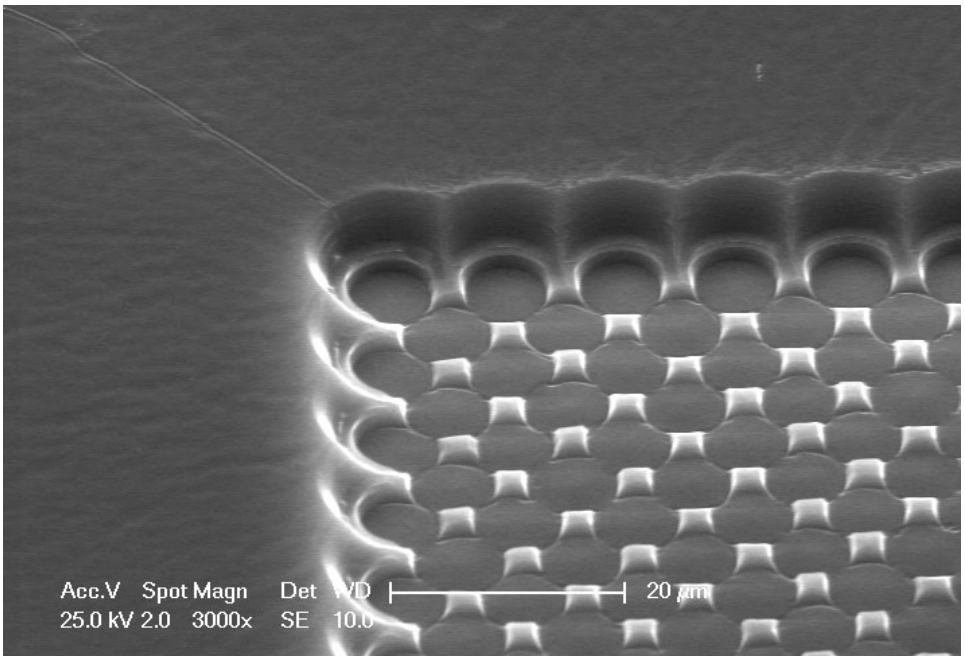

Figure 5.4: SEM image of etched PDMS. It is shown, that fabricating holes with a diameter of 5 μm using this mask design, proved to be impossible because the separation of the holes was lost due to the small spacing. The same holds for the spacing within the pattern of the 2 μm holes.

in the corners of the membrane. Also, since there was no experience with the fabrication of such large membranes, other size related factors also might have caused the rupture of the membrane.

To resolve the first problem, spacing between the holes was increased. Close inspection of the hill pattern in Fig. 5.4 reveals that the separation was only lost in the diagonal direction, which was the minimum spacing of the pattern. The maximum spacing (in x and y direction) was large enough to ensure separation of the holes. The adjacent hole resulting in the current minimum spacing was omitted, setting a new minimum spacing of 14 μm for the holes with a diameter of 5 μm, and a new minimum spacing of 10 μm for the holes with a diameter of 2 μm (Fig. 5.6).

The second issue had to be investigated, since it was not clear what caused it. This was done by making the membrane round and introducing a design variation in the diameter of the membrane: 10 mm and 15 mm (Fig. 5.7). The area of the largest membrane in the new design is around 80% of the original rectangular area, while the smallest membrane is only 35% of the original area. These variations will be suitable to point out size related issues during fabrication.

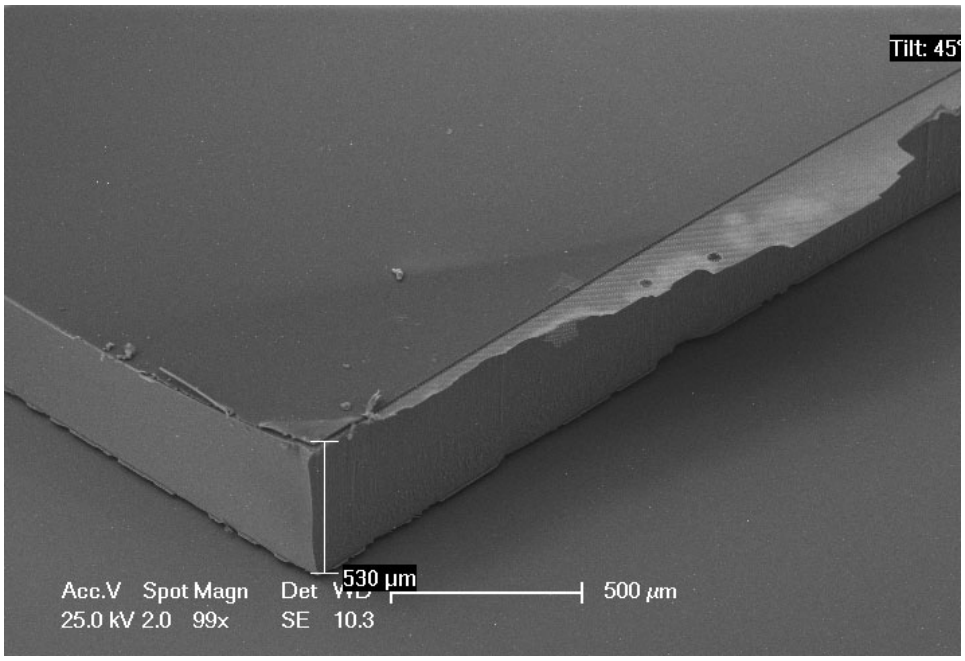

Figure 5.5: SEM image of a broken rectangular PDMS membrane. The reason of failure is either built up stress in the corners or the size of the membrane.

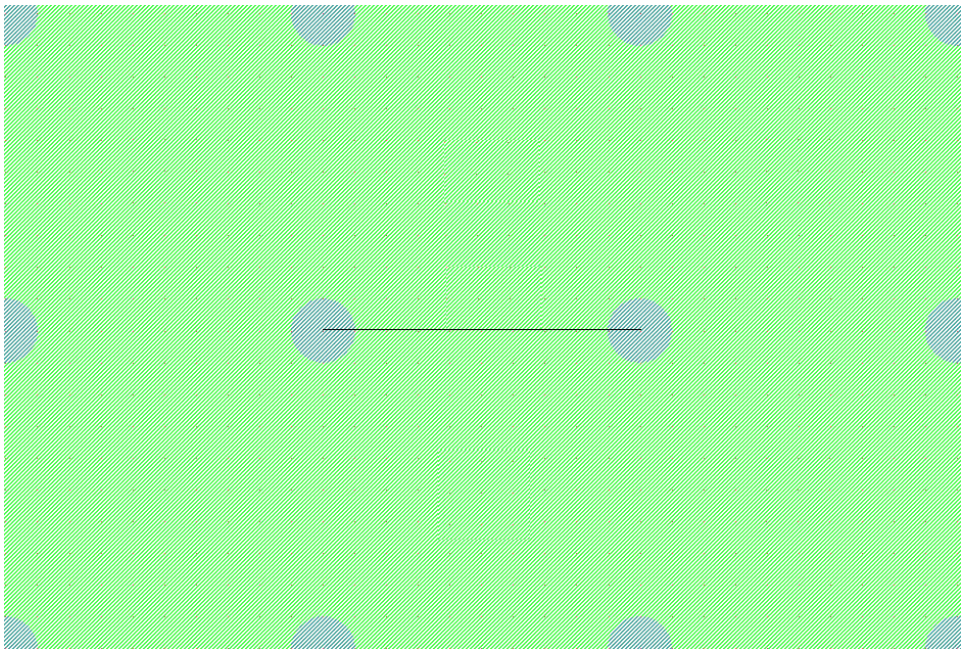

Figure 5.6: Close-up of the second version of the 2 μm hole pattern (HOLES). The black measurement bars indicate 10 μm.

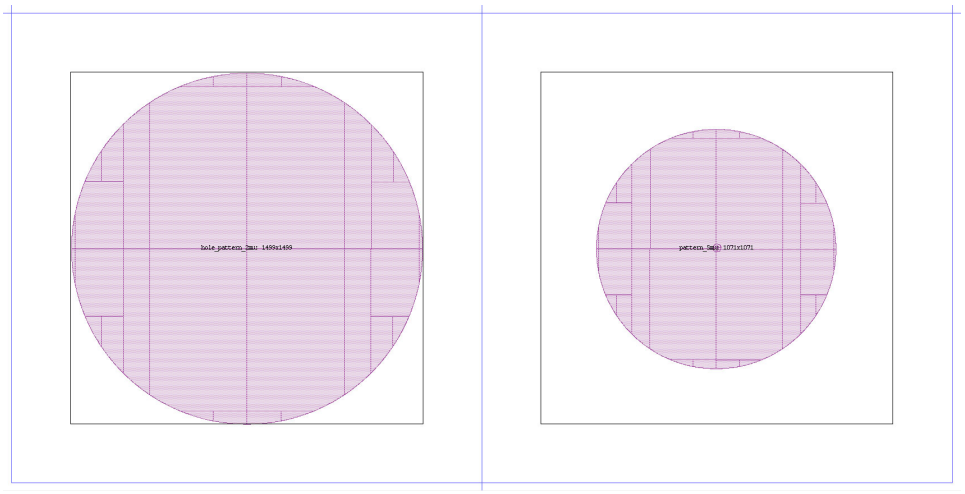

Figure 5.7: Mask design for circular membrane (BACK).

5.2 Fabrication of holes in PDMS

The methods for patterning the PDMS differ in the three process flows, proposed in Section 3.3. In this Section the results of all three patterning approaches are presented.

5.2.1 Etching

In the current process flow of Cytostretch, the PDMS layer is etched to open the bond pads. It would be efficient to etch the membrane holes at the same time. However, as described previously, the minimum feature size achievable with the current dry etching technique is about 12,6 μm, while the holes should have a diameter of about 5 to 8 μm. The minimum feature size to open the membrane is derived from the thickness of the membrane plus the maximum surface roughness (10 μm) divided by the isotropic ratio. This results in a minimum feature size of $(21/6) * 2 = 7$ μm. In practice the diameter will be larger due to a minimum feature size on the mask, which is typically around 2 μm for a contact aligner mask. For the bond pads this is acceptable, since they are very large (1400 by 800 μm^2), but the small holes cannot be fabricated by using only fluoride chemistry.

Implementing the new etching technique to make a perforated membrane does not only reduce the etching time with a factor five, but is also necessary to meet the specifications of the Cytostretch Skin device. However, due to lack of selectivity towards photoresist, a thick layer of photoresist was required as an etch mask (Fig. 5.8). Cracking now occurred because of the stress differences in the photoresist and PDMS, which was solved by including an aluminum layer as described in Section 4.2.3. This would

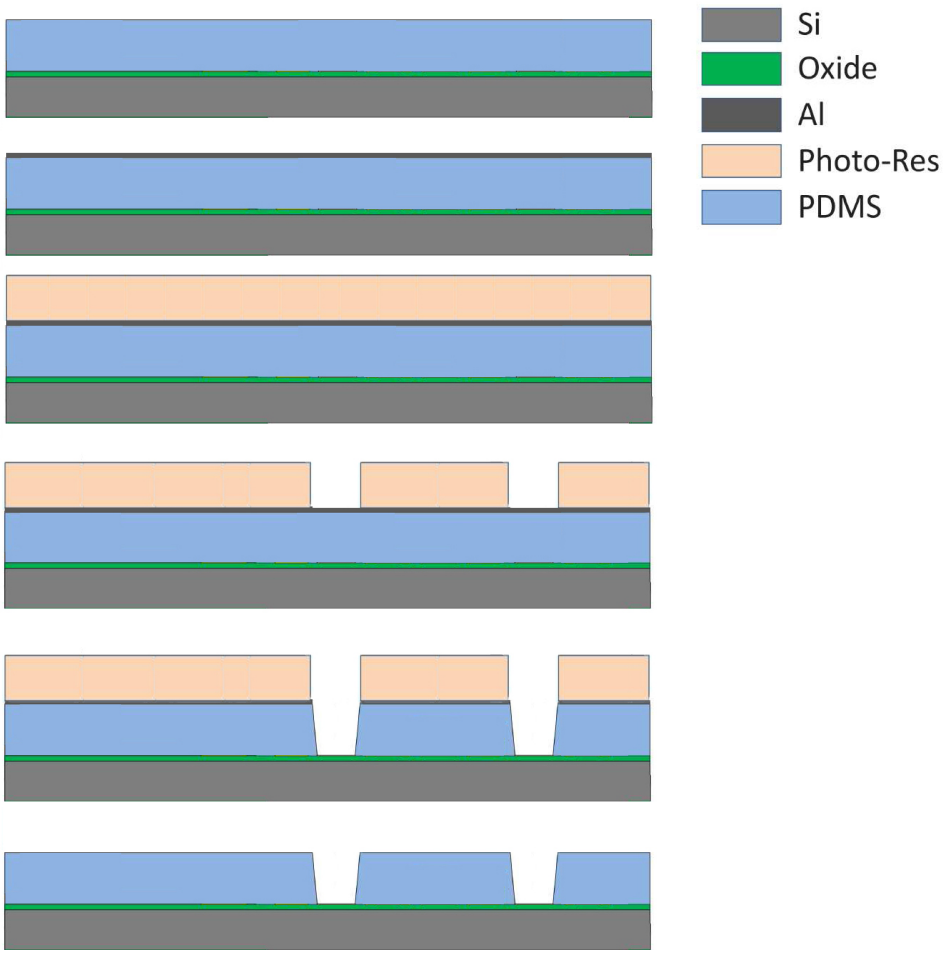

Figure 5.8: Process flow for the perforated membrane by selective removal of PDMS.

have introduced another patterning step for aluminum, but since the new etching technique is based on a chlorine chemistry, it simultaneously etches aluminum, eliminating the need for an additional mask step.

The dry etching method resulted in the desired pattern of holes in the case of the 5 μm design. Figure 5.9 shows the result after removal of the photoresist mask and the aluminum stress buffer. The wrinkles formed in the PDMS due to aluminum deposition are clearly visible. Furthermore, unlike in previous results, certain remnants are visible. These by-products might be the result of a chemical reaction of the aluminum in the Cl_2 and SF_6 plasma, as these remnants only occur on locations where aluminum was exposed to the plasma (Fig. 5.10). Although it was quite easy to wash these rings away, it is still an undesired side-effect.

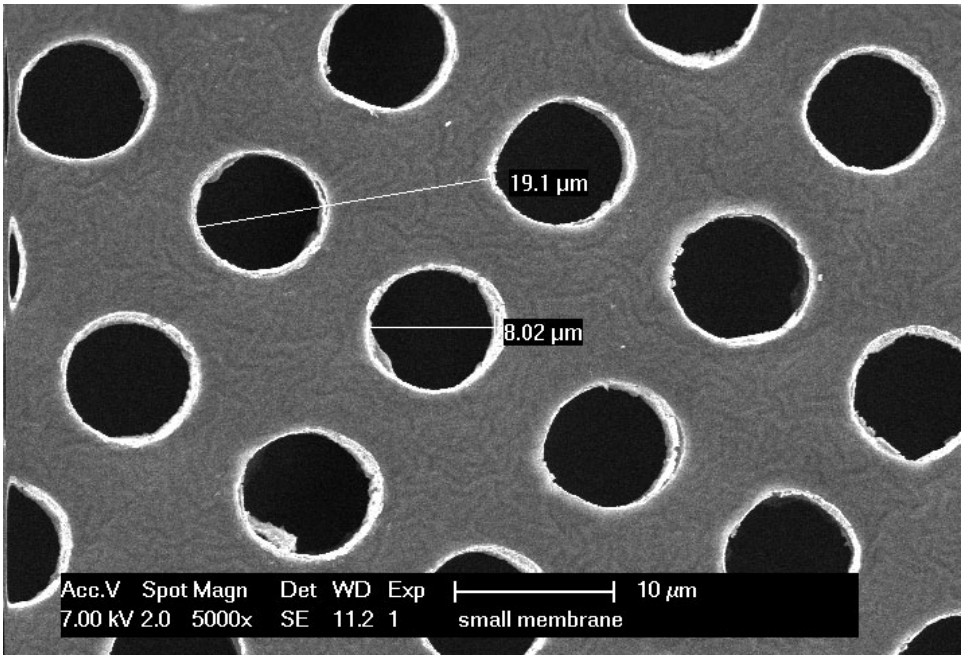

Figure 5.9: SEM picture of the result of the 5 μm hole design after dry etching.

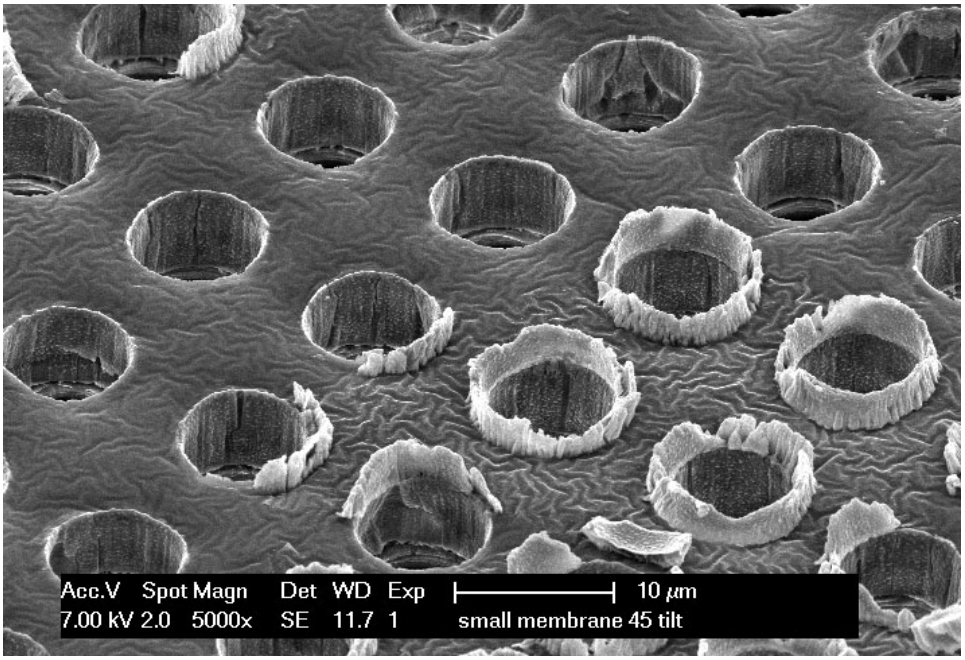

Figure 5.10: Etch remnants are clearly visible on this SEM picture. They seem to occur only on locations where aluminum was exposed to the plasma.

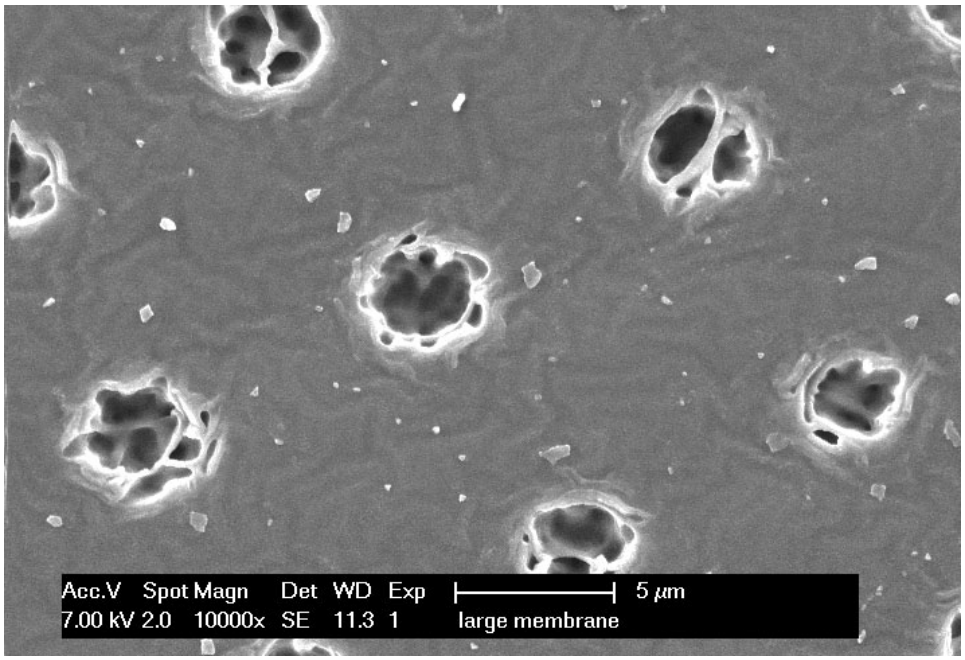

Figure 5.11: SEM picture of the result of the 2 μm hole design after dry etching. The holes are not fully open and do not have a well defined geometry.

Contrary to the results of the design of the larger holes, the design of the 2 μm hole pattern did not meet the requirements. The holes in this design were not etched deep enough, nor did they have well defined sidewalls (Fig. 5.11), not only at the edge of the wafer due to a lack of uniformity in the etching plasma, but at all locations throughout the wafer. It is believed that the high aspect ratio of the hole in the photoresist mask limits the number of chemical reactions and bombardments of the ions in the plasma. The ions cannot reach the PDMS surface well enough to etch with the same specifications as previously shown.

5.2.2 Selective deposition

As mentioned in Section 4.3.2, spin casting is usually done with SU8 or AZ9260. Since previous members in this research group had many difficulties with the removal of SU8, it was decided to discard SU8 as an option. AZ9260 however, has been used in the current process flow without any additional difficulties. The goal was to increase the resist thickness by at least a factor two, in order to minimize any unwanted coverage of PDMS (Fig. 5.12).

Although it was possible to fabricate resist pillars with a width of 5 μm and a height of 16 μm using a double spin procedure, most of these high aspect ratio pillars already broke off from the substrate during resist de-

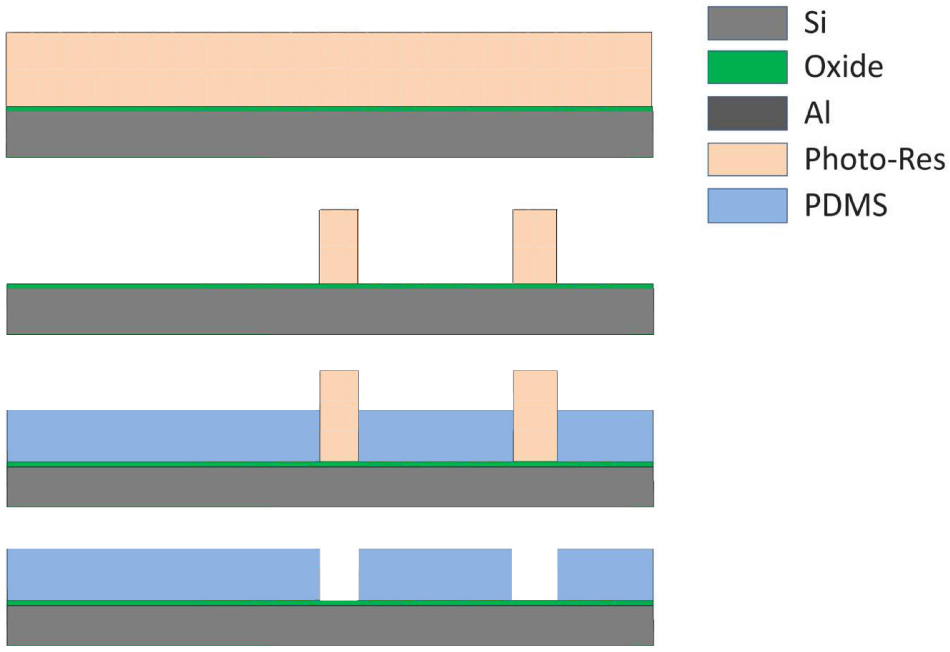

Figure 5.12: Process flow for the perforated membrane by selective deposition of PDMS.

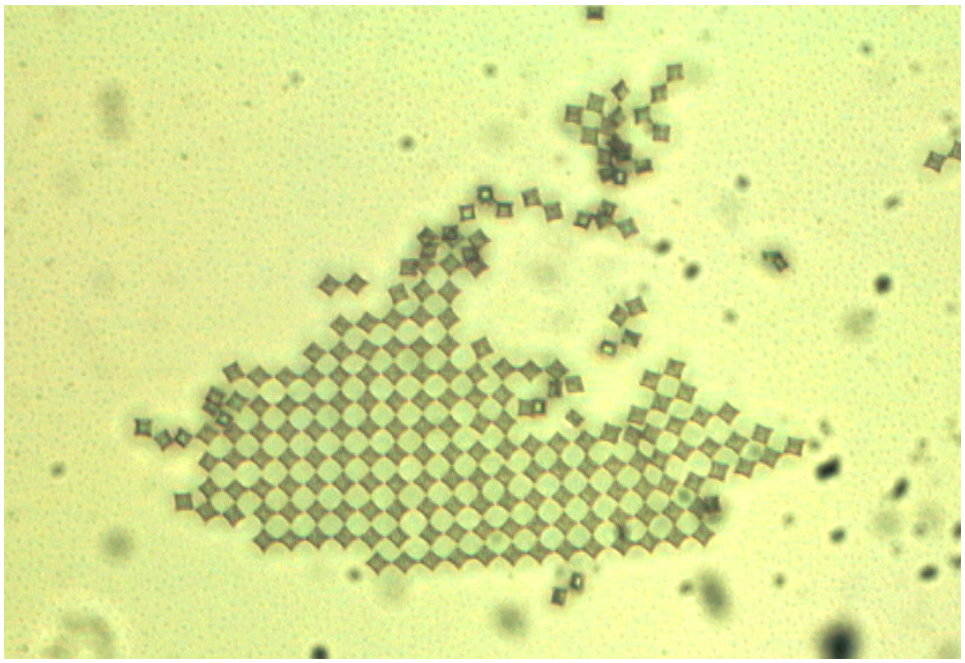

Figure 5.13: High aspect ratio resist pillars broke off during development.

velopment (Fig. 5.13). The remaining pillars broke off during PDMS spin casting. Since the patterning approach discussed in the previous Section proved more successful, no effort was made to improve this technique. Although it is believed that optimization of development will result in slightly better results, the forces associated with the high spin speed and thick layer of PDMS are likely to prevent this technique from having a high yield.

5.2.3 Selective deposition and etching

Selective deposition of PDMS did not prove to be a promising method to make holes in PDMS, but a combination deposition and removal of PDMS might reduce the etch time needed. On the other hand, such method makes the alignment of the etch mask more critical (Figure 5.14) and since PDMS is not allowed to be processed with the stepper, the accuracy is limited to the specifications of the contact aligner. A more significant problem was the remainder of what is believed to be cross linked photoresist due to UV components in the dry etching plasma, used for etching the PDMS (Figure 5.15). This resulted in 'foils' of PDMS on the bottom of the etched structures.

To overcome this residue issue, and assuming it is cross linked photoresist, it should be either removed or prevented. This cross linked photoresist can be removed using an oxygen plasma or NMP. An oxygen plasma attacks

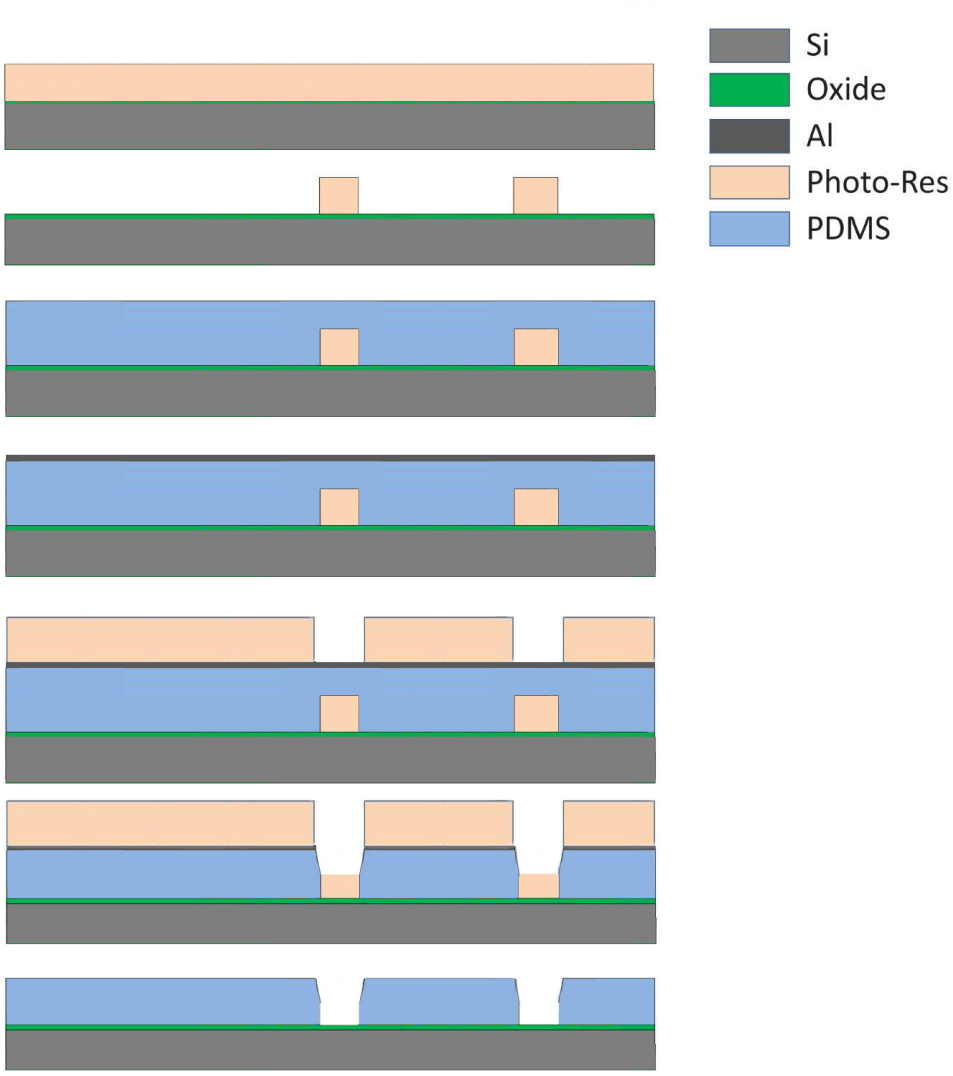

Figure 5.14: Process flow for the perforated membrane by selective deposition and selective removal of PDMS.

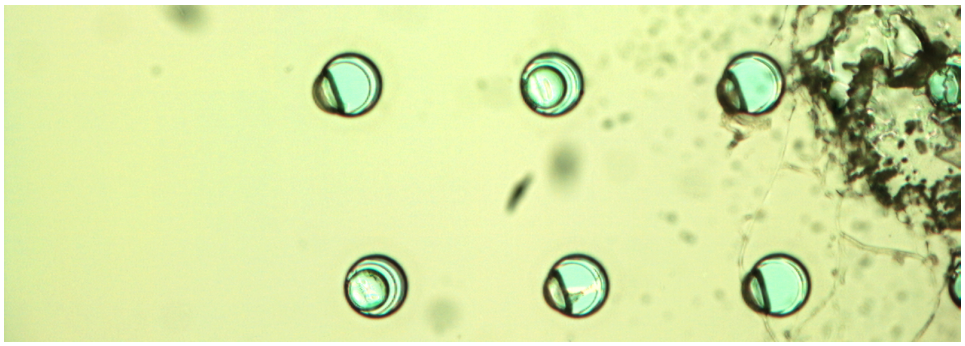

Figure 5.15: Patterned PDMS using a combination of spin casting and dry etching. Foils of what is assumed to be cross linked photoresist can be seen inside the holes where the PDMS is removed.

the PDMS and will alter the surface properties, resulting in microcracking, while NMP will etch the PDMS isotropically. Both of these methods will not be considered as options. To prevent cross linking of the photoresist by the dry etching plasma, an attempt was made to coat the photoresist pillars with a 250 nm thick layer of aluminum. However, the degassing of the photoresist was too high to be allowed in the sputter coater. Reducing the height of the photoresist is likely to resolve this problem.

5.3 Fabrication of the Cytostretch Skin device

In the previous Section, it is shown that fabricating holes with the desired dimensions is best done with the dry etching method. In this Section this approach is used to fabricate the complete Cytostretch Skin device. The final process flow is shown in Fig. 5.16.

5.3.1 Final process flow

First, a layer of low stress silicon dioxide is deposited on both sides of a 500 μm thick single sided polished p-type test wafer, with a thickness of 2 μm on the front side and 6 μm on the backside. The silicon dioxide on the backside is patterned with the BACK mask, which determines the size of the membranes. Next, the front side is spin coated with a 11 μm thick layer of PDMS. Before spin coating the 12 μm thick layer of photoresist that is used as an etch mask, an aluminum layer (with 1% silicon) is deposited on the PDMS to absorb the thermally induced stress. The thick layer of photoresist is now patterned with the HOLES mask and etched untill the silicon dioxide is reached. To release the membrane, the backside needs to be etched. In order to ensure clamping on the chuck in the deep reactive ion

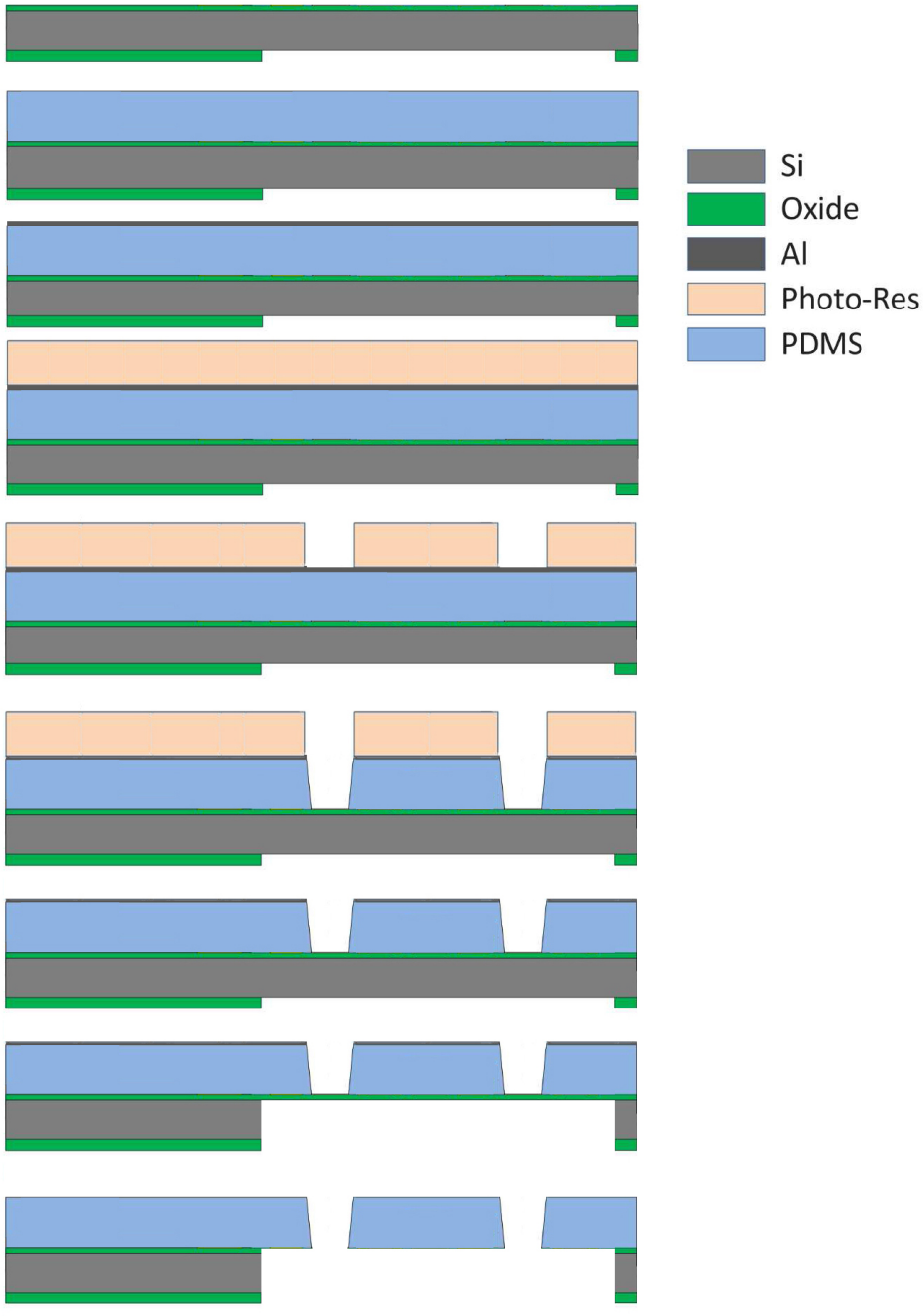

Figure 5.16: Final process flow for the Cytostretch Skin device.

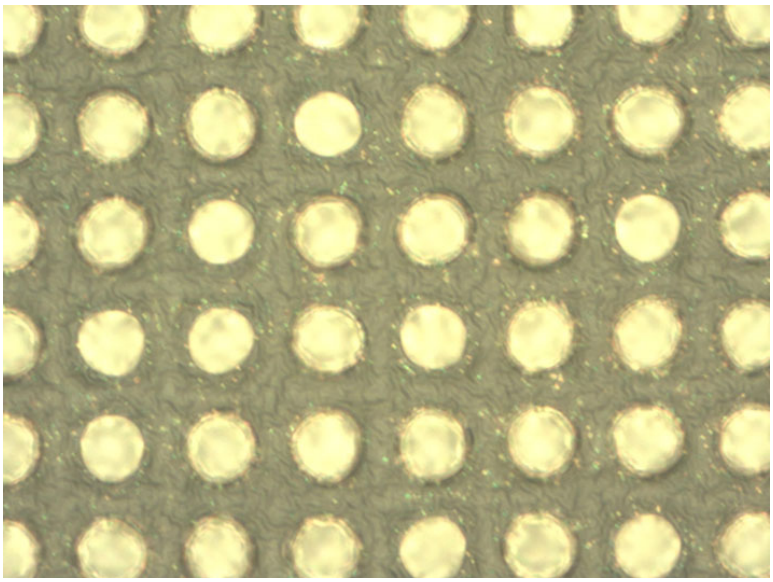

Figure 5.17: Light microscopy image of the 5 μm hole design after dry etching. The photoresist has been removed in aceton, the aluminum layer is still present.

etcher (DRIE), the photoresist is removed in aceton. However, the aluminium layer is left in place to prevent stiction - and thus rupture - of the PDMS membrane to the chuck or carrier wafer that can be used in the last phase of the DRIE (Fig. 5.17). The carrier wafer is used to prevent the chuck from being etched by the plasma in case a membrane fails. As an alternative for the carrier wafer, a 4 μm thick layer of aluminum can be deposited on top of the current aluminum layer to close the holes in the membrane and to support the thin membrane during DRIE. After these preperations the backside is etched using DRIE, which removes all silicon and lands on the front side silicon dioxide layer, releasing the membrane (Fig. 5.18). Finally, the aluminum layer is removed in PES and the silicon dioxide underneath the PDMS membrane is removed in BHF.

5.3.2 Final result

Although some membranes broke during etching of the silicon, the overall result was good (Fig. 5.19). SEM inspection of the back of the membrane showed a smooth surface and good geometry of the holes (Fig. 5.20). Some membranes contained superficial cracks in the surface of the PDMS (Fig. 5.21). These cracks are most likely copies from cracks in the silicon dioxide layer and do not cause the membrane to fail.

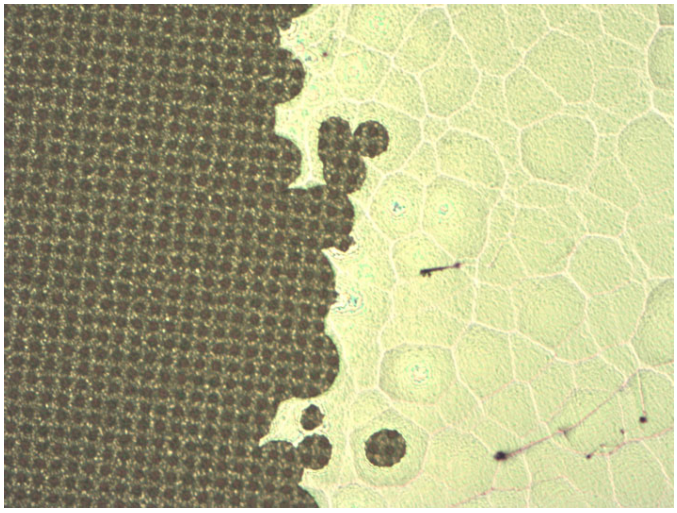

Figure 5.18: Light microscopy image of the 5 μm hole design during etching of the silicon substrate in order to release the membrane. The membrane is shown bottom up.

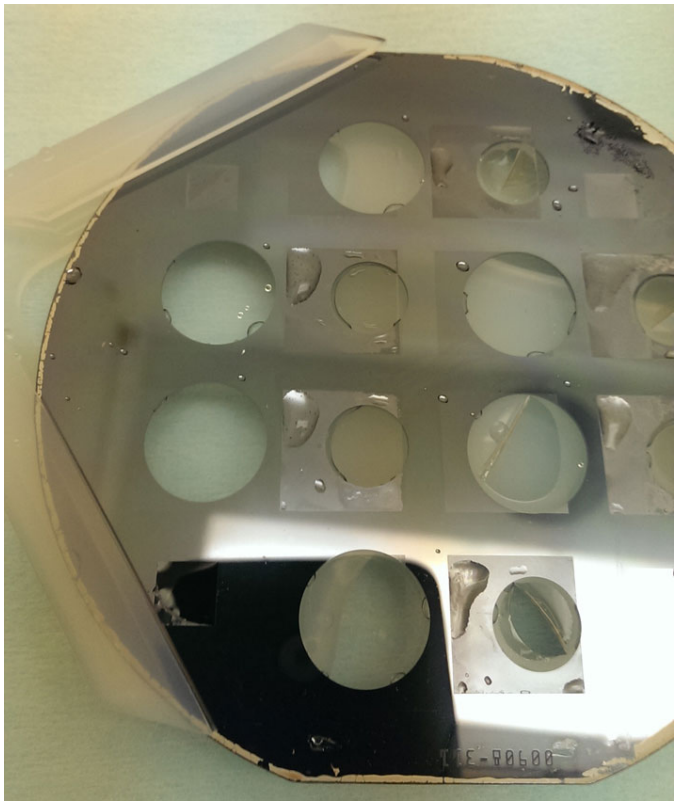

Figure 5.19: Picture of the Cytostretch Skin device after removal of the silicon dioxide. Some membranes broke during deep reactive ion etching.

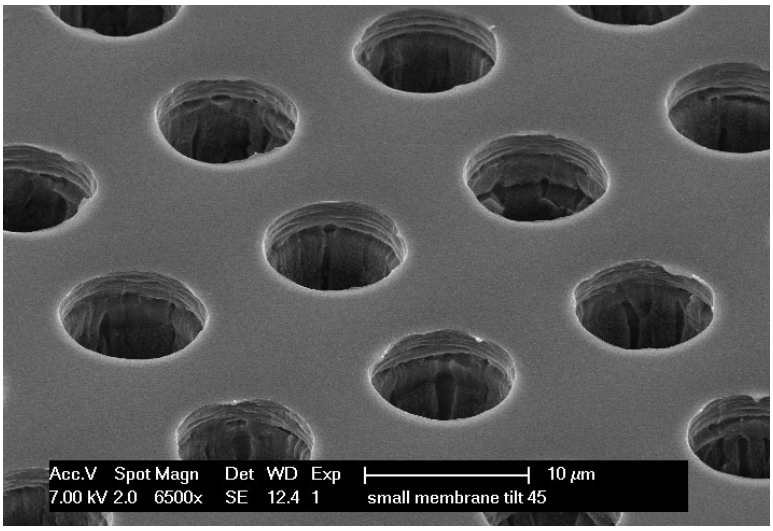

Figure 5.20: SEM image of the μm hole design bottom up after the final process step.

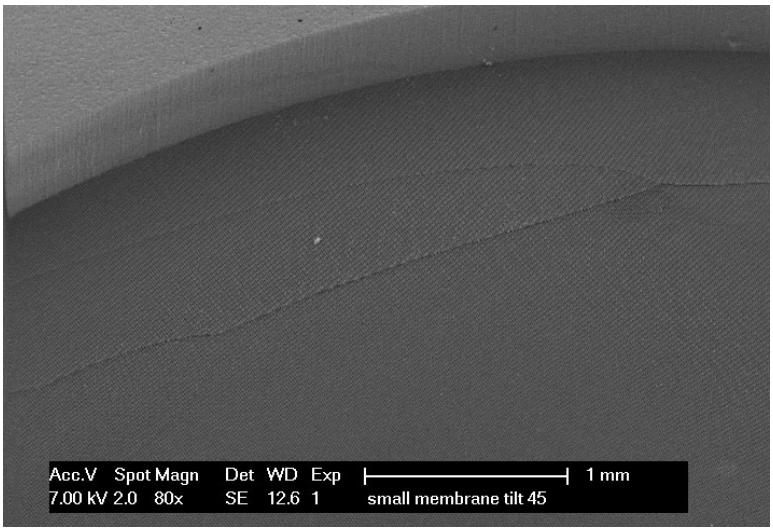

Figure 5.21: SEM images of Cytostretch Skin, seen from the backside of the wafer. Superficial cracks are present in the PDMS membrane.

Chapter 6

Skin on chip

Now that the first generation of the Cytostretch Skin device has been fabricated, its suitability for cell culturing had to be testing, in order to validate the device. In this Chapter, experiments are discussed in which cells were cultured on the device and the results were compared with cell plating on commercially available *transwells*. The Cytostretch Skin device was sterilized in ethanol for half an hour before coating and cell plating.

Due to an infection that was present in the stoves of the Department of Dermatology of the VU medical centre (VUmc), all of our experiments were contaminated and were aborted before completion. Nevertheless, some interesting results have been obtained, which will be presented in the next Sections.

6.1 Cell plating on a transwell

Transwells are perforated membranes, quite similar to the Cytostretch Skin deivce, but made out of different materials and not designed for stretching, aligning or the inclusion of electrodes. Before improving the skin model by stretching or aligning, Cytostretch Skin should give similar results of cell growth compared to transwells. In order to investigate whether the cells do not behave differently in the fabricated device, experimental results are compared with a standard transwell device. Preliminary experiments with plain slabs of PDMS without any pattern showed that the dermal fibroblasts were able to be cultured on the substrate. The biggest uncertainty in the fabricated device was not biocompatibility, but whether the holes would have a unwanted effect on the fibroblasts. To eliminate this uncertainty, a transwell with a small hole size was selected, in order to ensure that the results of the device would be compared to a membrane through which the cells would not fall.

Plating fibroblasts on a transwell is done without coating or special treatment. The cell culture results are shown in Fig. 6.1 and Fig. 6.2. As was

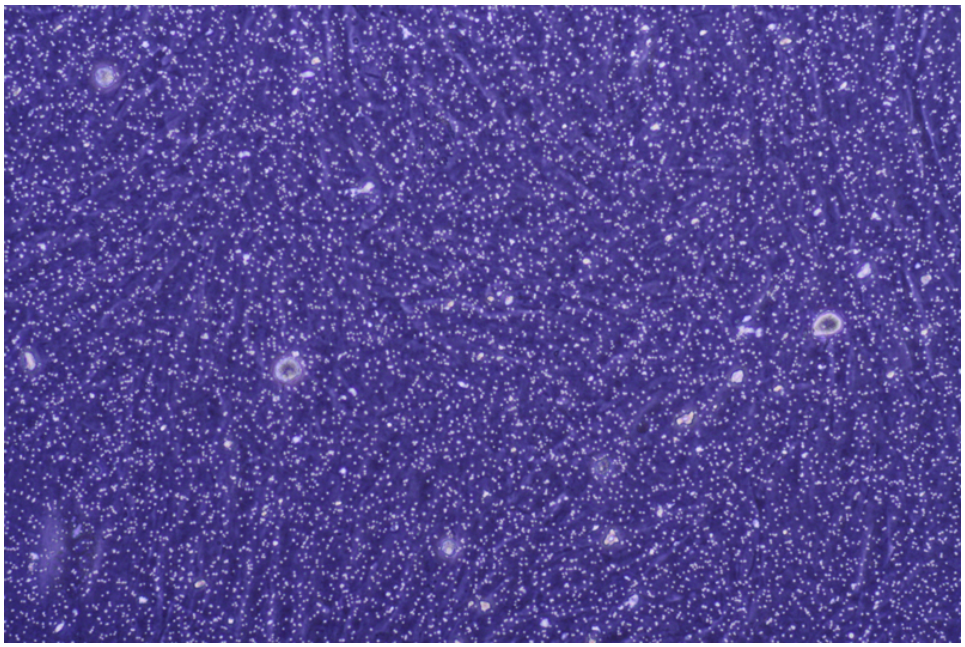

Figure 6.1: Light microscopy pictures of 0.4 μm transwell membranes with fibroblasts on day 1, at 5x magnification.

expected, the cells proliferated well and had good adherence to the transwell.

Since this experiment was aborted before plating keratinocytes, no immunohistochemical staining was performed. However, from previous experiments, it is known that results are expected to have similar results as the results shown in Fig. 2.3.

6.2 Skin growth on chip

PDMS is generally treated before plating cells, making the surface more hydrophilic to promote the adhesion of the cells [7, 41, 47]. The type of treatment depends on the type of cells plated. In this first experiment, two treatments were used and compared: fibronectin coating and UV treatment. For the fibronectin coating, a solution of 50 μg/mL was used and was kept at room temperature for one hour. The cell culture looked similar to the plating in the transwell, both on day 1 (Fig. 6.3) as well as on day 7 (Fig. 6.4).

The UV treatment was done for one hour using a UV lamp with a power of 10 to 40 Watt (uncertain). The UV changes the water contact angle, as previously described, but it was not possible to measure this at the medical facilities. The water contact angle was still quite high and is estimated at 90°. The cell culture looked similar to the plating in the transwell, both on day 1 ((Fig. 6.5) and on day 7 (Fig. 6.6).

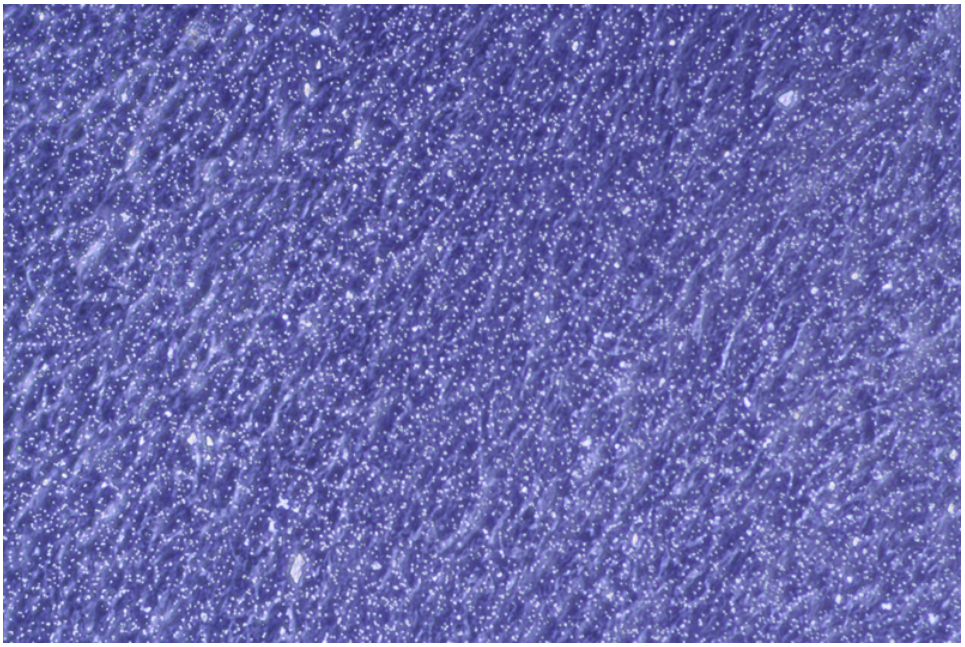

Figure 6.2: Light microscopy pictures of 0.4 μm transwell membranes with fibroblasts on day 7, at 20x magnification.

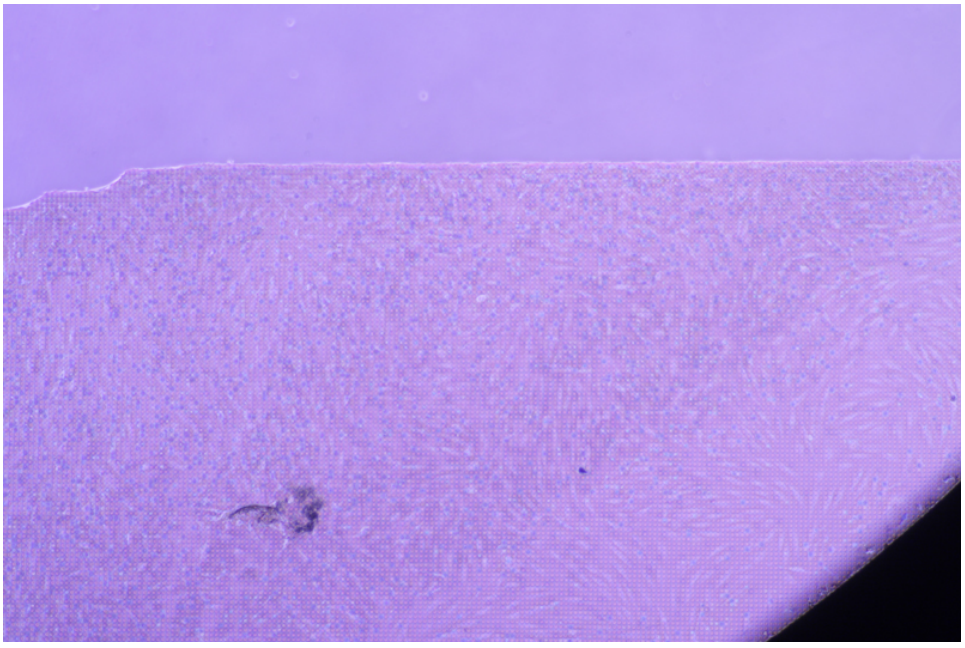

Figure 6.3: Light microscopy pictures of fibronectin coated the Cytostretch Skin device with fibroblasts on day 1 at 5x magnification.

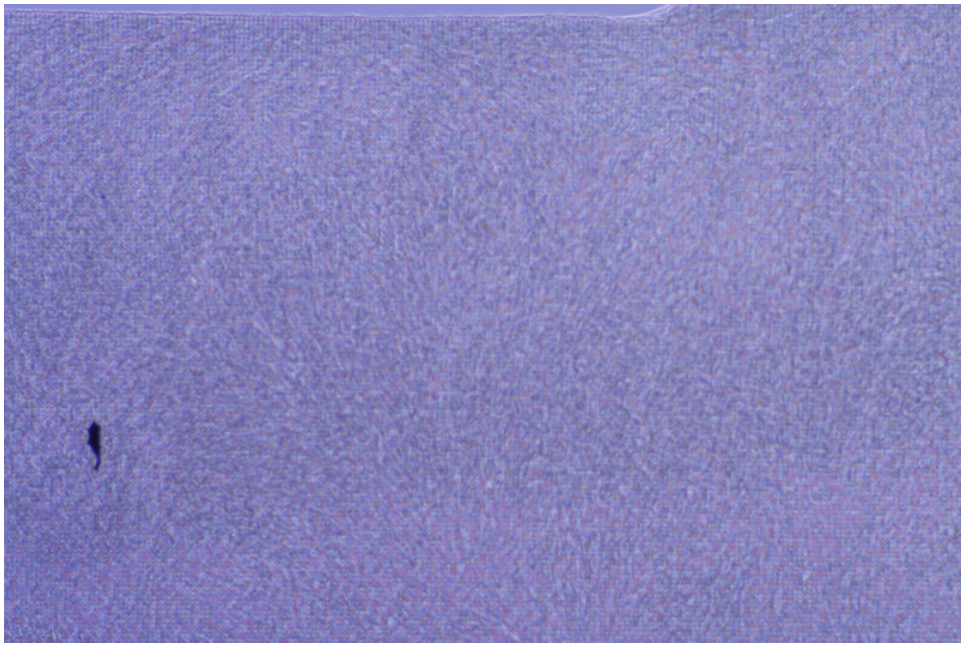

Figure 6.4: Light microscopy pictures of fibronectin coated the Cytostretch Skin device with fibroblasts on day 7 at 5x magnification.

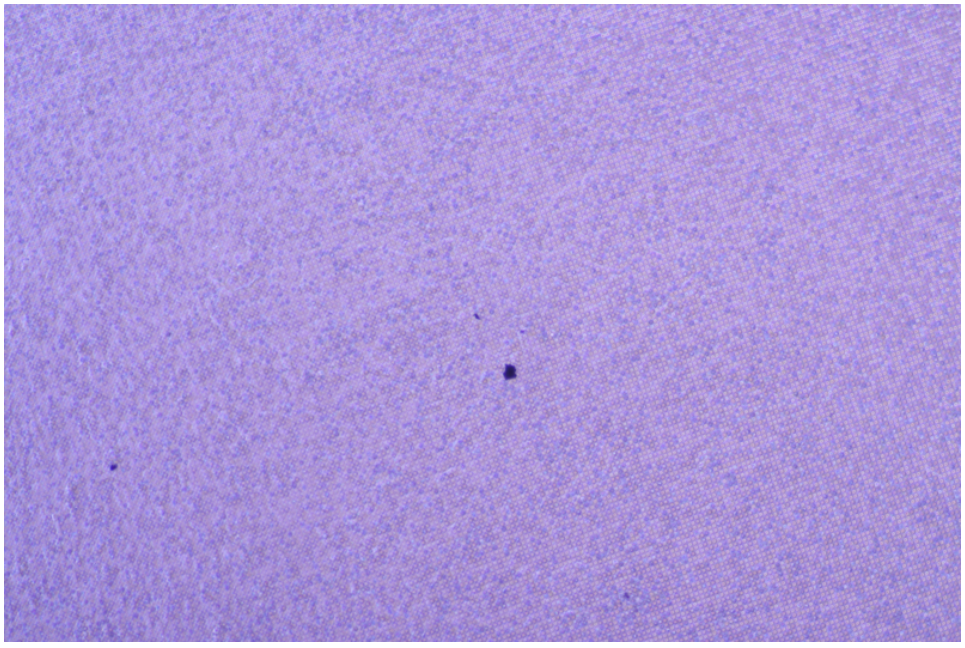

Figure 6.5: Light microscopy pictures of UV treated the Cytostretch Skin device with fibroblasts on day 1 at 5x magnification.

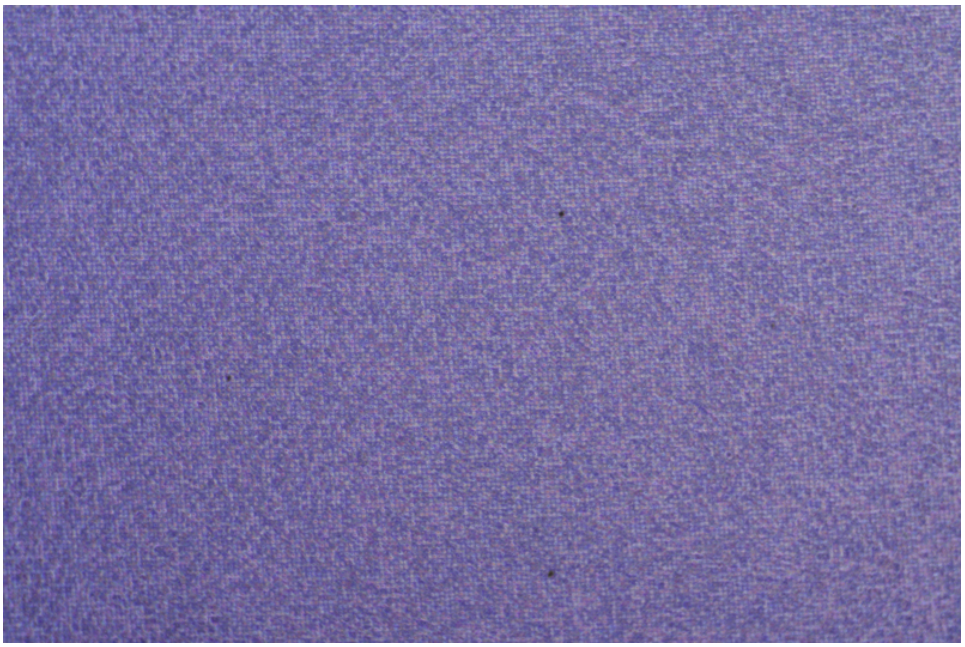

Figure 6.6: Light microscopy pictures of UV treated the Cytostretch Skin device with fibroblasts on day 7 at 5x magnification.

The figures above do not have an optimal focus due to the interference caused by the substrate, yet still it is clear that cell proliferation is present on both substrates. All initial cell concentrations were equal and no significant differences were visible on the transwell and both Cytostretch Skin membranes. Since the fibroblast feeder layers showed good proliferation, they were seeded with keratinocytes after 4 weeks to start formation of an epidermal layer. After 5 weeks, the experiment was terminated because of an infection in the cell culture. This infection was present in the lab prior to the introduction of the Cytostretch Skin device, the device is not suspected to be the cause of this contamination. After terminating the experiment, the Cytotretch Skin model was fixated and embedded to make cross sections for immunohistochemical staining. Figure 6.7 shows the results, which are complex to interpret. A large number of aligned cell nuclei can be found just above the membrane of the device. This might have been the start of the development of an epidermis layer. Also, when compared to Fig. 2.3, which is shown at the same magnification, the layer has approximately the same thickness as the epidermis layer on the MatriDerm®. However, since the MatriDerm®model has a substrate of collagen, the number of fibroblasts and their spatial organization might be different from the Cytostretch model. In the latter the cells must produce their own extracellular matrix. Additional staining has to be done to confirm the spatial arrangement of the fibroblasts and the keratinocytes. In addition, since the experiment is

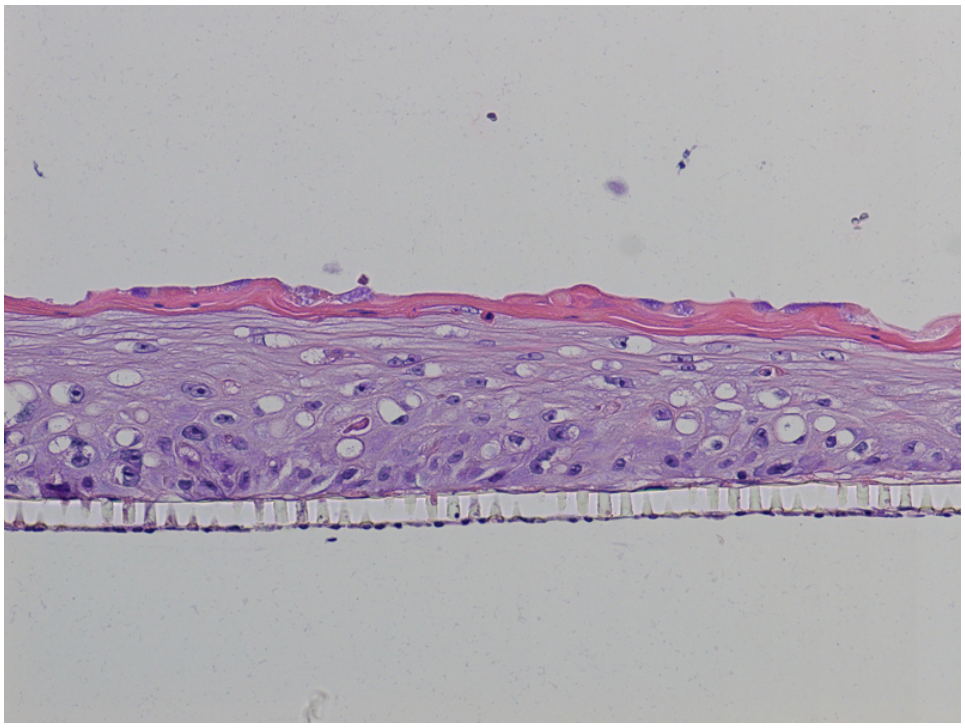

Figure 6.7: Immunohistochemical staining of Cyotstretch Skin.

terminated in an early stage, future results might differ as a result of more progressed tissue development.

It should also be noted that some nuclei seem to be visible beneath the porous membrane. This could indicate that cells have fallen through or have migrated. However, it is not certain these are nuclei, they might also be accumulated stained proteins.

Further experiments will have to be done to review epidermal cell growth on top of these dermal fibroblasts and endothelial cell growth on the bottom of the membrane. For now, it is concluded that the device behaves as intended.

Chapter 7

Discussion

The results presented in the previous Chapters give rise to several discussions. The most significant issues are discussed in this Chapter.

7.1 Chemical reactions during etching

As shown in Figure 4.1, the backbone of polydimethylsiloxane (PDMS) consists of alternating atoms of silicon and oxygen with two methyl groups at every silicon atom. Using chlorine to etch PDMS makes sense from a chemical point of view, since the starting material for producing PDMS is chlorine-based: dimethyldichlorosilane or $(CH_3)_2SiCl$. Therefor, in this Section it is hypothesized that a chlorine based etch chemistry reverses this reaction and splits the PDMS back in small dimethylchlorosilane groups.

Dimethyldichlorosilane is made of silicon and methyl chloride and is a clear liquid at room temperature, with a boiling point around 70°C. PDMS is made by adding water to dimethyldichlorosilane, which reacts as [16]

$$nSi(CH_3)_2Cl_2 + nH_2O \rightarrow [Si(CH_3)_2O]_{\mathrm{n}} + 2nHCl \tag{7.1}$$

and forms a chain of n dimethylsiloxane groups under the formation of two times n hydrogen chloride molecules. The first chlorine etch experiments that were conducted as described in Section 4.5.3 were done with chlorine (Cl_2) in combination with hydrogen bromine (HBr). The reaction that would take place is hypothesized to be

$$[Si(CH_3)_2O]_{\mathrm{n}} + nCl_2 + 2nHBr \rightarrow nSi(CH_3)_2Cl_2 + nH_2O + nBr_2 \tag{7.2}$$

in which the dimethyldichlorosilane is heated above its boiling point due to the kinetic energy of the incoming ions.

Assuming this reaction takes place, preferably, the dimethyldichlorosilane would be split further into silicon and methyl chloride. Methyl chloride

is in its gas phase at room temperature and will thus quickly move to the outlet of the plasma chamber. Fluorine has a good reaction with silicon, together forming the gas silicon tetrafluoride (SF_4). When sulfur hexafluoride (SF_6) is used to etch silicon the reaction

$$4SF_6 + Si + e,^- \rightarrow 4SF_5,^- + SiF_4 \tag{7.3}$$

takes place where both products are volatile. However, it is unknown whether this reaction will occur, since it is also possible that the fluorine reacts directly with the PDMS.

Without measuring the reaction species in the outlet of the plasma chamber it is impossible to determine the precise reaction. The chemical interactions are worthwhile to investigate, in order to optimize the etching process.

7.2 Stop layer for dry etching with Cl_2 and SF_6

As most materials used in microfabrication are etched in either a chlorine or a fluorine plasma, it is hard to find a material towards which a combined plasma has good selectivity. This introduces two problems: lack of a good masking layer and lack of a good stop layer. The first problem is relatively easy to resolve by increasing the thickness of the masking layer. This may not be ideal, because increasing the thickness of the mask decreases the accuracy of the pattern. However, it provides for a workable solution since the inaccuracy can be compensated for in the design of the mask.

The lack of a good stop layer is more complex. In the process flow of the perforated membranes this does not introduce a problem, but when opening the bond pads in the process flow of the first Cytostretch device (Fig. 3.1), the metal of the bond pad will be etched fast, because of the chlorine component in the plasma. To deal with this problem it is possible to time the process precisely with a controlled etch speed or to switch to a fluorine only plasma just before reaching the bond pad. The first solution introduces uncertainty, as the transparency of PDMS makes it hard to visually confirm whether the bond pad is etched open. The second solution limits the quality of the etching, as it will etch more isotropically and will introduce surface roughness, making a long overetch necessary.

To optimize the etch technique, a more selective layer has to be found which has a lower etch rate in both chlorine as well as fluorine chemistry.

An alternative to using a stop layer is to incorporate a sacrificial layer, making it acceptable to have a poorly defined endpoint detection. In this case a thick layer of aluminum or photoresist could be used. Since the etch speed is well above 1 μm/min and thus a layer of at least a few micrometers

is necessary, photoresist is the preferred material. However, cross linking of the photoresist layer will become a problem, as the process is equal to the combination of spin casting and etching, as described in Section 5.2.3.

7.3 Efforts on fabrication methods

From the results shown in Chapter 5 it is clear that the introduced dry etching method is the best method for making small features with high aspect ratio's in PDMS. In fact, the other tested methods did not meet the required specifications. It is noted here that the amount of effort put in the three methods (i.e. selective removal of PDMS, selective deposition of PDMS and a combination of both) is not equal. Selective deposition is investigated thoroughly, but without good results. Etching of PDMS brought such promising results, that it was decided to only briefly experiment with the combination of patterning approaches. First results of the experiments confirmed the current focus of the research project. However, the option of combining the techniques of spin casting and dry etching is not ruled out entirely, especially since a sacrificial landing layer might be necessary (Section 7.2).

7.4 Coating PDMS to promote cell adhesion

Cell adhesion to PDMS has been researched in the past and appears to be cell type dependent [24, 60]. In Chapter 6 it has been shown that dermal fibroblasts adhere to UV treated or fibronectin coated PDMS. In previous research the cardiomyocytes were plated after exposing the substrate to an oxygen plasma and coating it with fibronectin. Both UV treatment and oxygen plasma cause the PDMS to form silanol groups at the surface of the PDMS and make the surface more hydrophilic. Fibronectin seems to adhere better to hydrophilic surfaces, but whether this is because of better bonding to the PDMS or better spread of the liquid coating remains unclear. To investigate this further, fluorescent fibronectin could be used to look into the spread and adherence on treated surfaces, compared to non-treated surfaces.

Another method to promote the adhesion of extracellular matrix proteins is by using aminopropyltrimethoxysilane [58]. Aminopropyltrimethoxysilane provided this research group with promising results, which yet have to be published.

7.5 Membrane thickness

As stated before, the thickness of the perforated membrane in this thesis was on average 11 μm. Limited by the spin speed, thinner membranes were impossible to fabricate without diluting the PDMS or changing the mixing

ratio between the two components. However, Cytostrectch Skin is likely to benefit from a membrane that is as thin as possible, as it would further replicate the physiological environment - where no membrane is present at all. Eliminating the substrate is not an option since the cells have to be plated on something, but (biological) degradable materials could be interesting to develop. For a device that has the constraint of having a PDMS membrane, the aim should be to make the membrane as thin as possible.

Fabricating mass producible perforated membranes using microfabrication technologies, as presented in this thesis, allows for very thin membranes compared to process flows that involve (manual) membrane transfer steps. In both methods diluting PDMS can result in thinner membranes, but transferring PDMS from one substrate to another introduces handling problems, which limit the membrane thickness. Using a perforated polymer that is released by back-etching eliminates such handling problems and allows for thinner membranes, limited only by its own elasticity.

7.6 Other applications

Since polymers are relatively new in microfabrication, there is a lack of good process technologies when compared to more standard materials, like silicon. The introduction of the new dry etching method described in this thesis will allow engineers to use PDMS more frequently, even when small feature sizes are required. The results of this thesis are valuable for Cytostretch Skin. Moreover, the results will exceed this specific application, impacting PDMS process technology in general.

Chapter 8

Conclusion

From the research presented in this thesis, certain insights are gained and several conclusions can be drawn.

- In order to fabricate small features in polydimethylsiloxane (PDMS), etching with a chemistry of both Cl_2 and SF_6 is a useful method, even though selectivity towards other materials explored so far is limited.
- Using the Cl_2 and SF_6 chemistry, the design requirements for the Cytostretch Skin device are met. More precisely, the device
  - has a perforated membrane with a hole diameter in the range of 5 to 8 μm;
  - has a membrane diameter of at least 10 mm;
  - allows for cell plating on both sides of the membrane.

  Also, perforation of the membrane is a modular step that can be in- or excluded in the design of the previously developed Cytostretch. It does not require any additional mask steps and is suitable for mass production.
- The results from skin growth on the Cytostretch Skin device are preliminary, but promising. Cell proliferation seems to be comparable to cell proliferation in other *in vitro* skin tissue models.
- Spin casting is not likely to be a useful approach, either due to problems with removing the cast after spin casting using SU8 or due to failure of the cast during development and spin coating PDMS using AZ9260.
- The combination of spin casting and etching is promising, especially considering there is no good stop layer available for the etching chemistry of Cl_2 and SF_6.

- Using a buffer layer of aluminum on PDMS is a good method to prevent thick photoresist layers to crack due to the difference in coefficient of thermal expansion of the different materials.
- Membranes should be round and not rectangular.
- Although promising new techniques are being developed to work with PDMS, it remains a challenging material to process in a microfabrication cleanroom environment.

Chapter 9

Recommendations

To put the results found during the research described in this thesis to use, additional research is recommended:

- Incorporate the etching technique presented in this thesis in a full Cytostretch device with electrodes and alignment topology;
- Investigate the products released during dry etching of polydimethylsiloxane (PDMS) using a chemistry of Cl_2 and SF_6, in order to determine the chemical reactions in the plasma;
- Study the influence of the membrane thickness on the communication between the endothelial and dermal cell layers;
- Develop a more open membrane design to minimize the effect of the membrane in the Cytostretch Skin model. This designed membrane should be a support layer in the cell plating stage, and being barely present in the drug testing phase. Such design can be realized with (partly) biodegradable polymers and/or a fishnet layout;
- Research the adhesion of extra cellular matrix proteins and cell types on PDMS.

Appendix A

Detailed process flow

Delft Institute of Microsystems and Nanoelectronics

TU Delft

ECXXXX

FLOWCHART

FRONTSIDE PROCESSING

CR100

Step 1. Cleaning

- HNO_3 (100%) @ RT – 10 min
- H_2O – 5 min (or until water reaches 5MΩ)
- HNO_3 (65%) @ 110˚C – 10 min
- H_2O – 5 min (or until water reaches 5MΩ)
- Dry and rinse in Semitool

Step 2. Low stress LPCVD Oxide

- Novellus
- 2 μm
- Program: "Zerostress"

Step 3. Measurement of oxide thickness

- Leitz MPV-SP tool
- Program: "Th. SiO2 on Si, >50nm auto5pts"

BACKSIDE PROCESSING

Step 4. Low stress LPCVD Oxide

- Novellus
- 6 μm
- Program: "Zerostress"

FRONTSIDE PROCESSING

Step 5. Photoresist

- EVG 120 Coater-Developer
- 1.4 μm positive SPR3012
- Program: "CO_SPR3012_ze"

Step 6. Exposure of Alignment Markers

- EVG 420 Contact Aligner
- Hard contact, 10 sec
- Mask: Alignment markers

Step 7. Development

- EVG 120 Coater-Developer
- Program: "dev_sp"

Step 8. Etch oxide

- Drytek
- 4 min
- Program: "std_oxide"

Step 9. Strip resist

- Tepla

- Pogram: “#1”

Step 10. Cleaning
- HNO_3 (100%) @ RT – 10 min
- H_2O – 5 min (or until water reaches 5MΩ)
- HNO_3 (65%) @ 110˚C – 10 min
- H_2O – 5 min (or until water reaches 5MΩ)
- Dry and rinse in Semitool

BACKSIDE PROCESSING

Step 11. Photoresist
- EVG 120 Coater-Developer
- 3 µm positive 3017M, no edge beat removal
- Program: “CO_3017M_3um_no-EBR”

Step 12. Exposure of mask BACK
- EVG 420 Contact Aligner
- Hard contact, 20 sec
- Mask: P3285_V2 – BACK_2

Step 13. Development
- EVG 120 Coater-Developer
- Program: “dev_sp”

Step 14. Etch oxide
- Drytek
- 12 min
- Program: “std_oxide”

Step 15. Strip resist
- Tepla
- Pogram: #1

Step 16. Cleaning
- HNO_3 (100%) @ RT – 10 min
- H_2O – 5 min (or until water reaches 5MΩ)
- HNO_3 (65%) @ 110˚C – 10 min
- H_2O – 5 min (or until water reaches 5MΩ)
- Dry and rinse in Semitool

Step 17. Photoresist for backside protection
- EVG 120 Coater-Developer
- 3 µm positive 3017M, no edge beat removal
- Program: “CO_3017M_3um_no-EBR”

MEMS Lab

Step 18. PDMS preparation

- Use weighing scale to mix PDMS curing agent (by pipette) and elastomer (by pooring) in a ratio of 1:10 in a plastic disposable cup

CR100

Step 19. PDMS mixing and degassing

- Thinky Speedmixer
- Program: #1

FRONTSIDE PROCESSING

Step 20. Spin on PDMS

- Lanz Manual Spinner (covered with aluminum foil)
- 5500 RPM
- Program: #15

Step 21. Bake PDMS

- Memmert Oven using dedicated carrier
- 30 min @ 90ºC

BACKSIDE PROCESSING

Step 22. Clean

- Lanz Manual Spinner (covered with aluminum foil)
- During spinning (3200 RPM):
    - Dispense acetone to remove photoresist and lift-off PDMS at backside, pay extra attention to the edges of the wafer
    - Dispense IPA to remove last particles
- Program: #4
- Dry on single wafer spinner

Step 23. Extensive inspection of backside

- Extra focus on edges
- Removal of particles if necessary

FRONTSIDE PROCESSING

Step 24. Dehydration bake

- Memmert Oven using dedicated carrier
- 30 min @ 90ºC

Step 25. Aluminum (1% silicon) deposition (stress absorption layer)

- Sigma
- 250 nm @ RT with periodic cooling
- Program: “AlSi_for_Organics”

Step 26. HMDS
- Manual HMDS
- 10 min

Step 27. Photoresist
- Lanz Manual Spinner (covered with aluminum foil)
- 12 µm AZ9260,
- 950 RPM

Step 28. Soft Bake
- Memmert Oven using dedicated carrier
- 30 min @ 90ºC

Step 29. Cool down
- At room temperature
- 15 min

Step 30. Exposure of holes-mask
- EVG 120 Contact Aligner
- Hard contact, 50 sec
- Mask: P3285_V3 – HOLES_V2

Step 31. Post Exposure Bake
- Memmert Oven using dedicated carrier
- 30 min @ 90ºC

Step 32. Cool down
- At room temperature
- 15 min

Step 33. Development
- Wetbench
- AZ400K:H_2O - 1:2, 2 min

Step 34. Al & PDMS etching
- Omega
- Cl_2:SF_6 – 30:10 SCCM
- Program: “PDMS”

Step 35. Clean resist
- Wetbench
- Aceton & IPA
- Dry on single wafer spinner

Step 36*. Dehydration bake
- Memmert Oven using dedicated carrier
- 30 min @ 90ºC

Step 37*. Aluminum (1% silicon) deposition (anti-stiction and chuck protection layer)
- Sigma
- 2500 nm @ RT with periodic cooling
- Program: "AlSi_for_Organics"

BACKSIDE PROCESSING

Step 38: Deep etch for membrane release
- Adixen AMS100
- ~ 100 min (check periodically near endpoint)
- Program: "Mapperspeed"

SAL

Step 39: Removal of aluminum
- PES
- 6 min

Step 40: Removal of oxide
- BHF
- 6 min

* Not necessary if a carrier wafer is used for deep etching.

Bibliography

[1] Deniz Armani, Chang Liu, and Narayan Aluru. RE-CONFIGURABLE FLUID CIRCUITS BY PDMS ELASTOMER. In *Micro Electro Mechanical Systems*, pages 222–227, 1999.

[2] Celine Auxenfans, Julie Fradette, Charlotte Lequeux, Lucie Germain, and Fabienne Braye. Evolution of three dimensional skin equivalent models reconstructed in vitro by tissue engineering. *European Journal of Dermatology*, 19(2):107–113, 2009.

[3] B Balakrisnan, S Patil, and E Smela. Patterning PDMS using a combination of wet and dry etching. *Journal of Micromechanics and Microengineering*, 19(4):047002, April 2009.

[4] S. Bhattacharya, a. Datta, J.M. Berg, and S. Gangopadhyay. Studies on surface wettability of poly(dimethyl) siloxane (PDMS) and glass under oxygen-plasma treatment and correlation with bond strength. *Journal of Microelectromechanical Systems*, 14(3):590–597, June 2005.

[5] Clemens Antoni Van Blitterswijk, Lorenzo Moroni, Jeroen Rouwkema, Ramakrishnaiah Siddappa, and Jérôme Sohier. *Tissue Engineering - An introduction*. Elsevier B.V., 2008.

[6] Esther Boelsma, Susan Gibbs, Claudine Faller, and Maria Ponec. Characterization and Comparison of Reconstructed Skin Models: Morphological and Immunohistochemical Evaluation. *Acta Derm Venereol*, 80:82–88, 2000.

[7] Nicolai Böker. Prototyping of a Stretchable Microelectrode Array for Cardiotoxicity Drug Screening. Master's thesis, Delft University of Technology, 2009.

[8] Jeffrey Borenstein. NIH Public Access. *IEEE Pulse*, 2(6):28–34, 2011.

[9] Jean-michel Bourget, Maxime Guillemette, Teodor Veres, François A Auger, and Lucie Germain. Alignment of Cells and Extracellular Matrix Within Tissue-Engineered Substitutes. In *Advances in Biomaterials*

Science and Biomedical Applications References, chapter 14, pages 365–390. InTech, 2013.

[10] Ned Bowden, Wilhelm T. S. Huck, Kateri E. Paul, and George M. Whitesides. The controlled formation of ordered, sinusoidal structures by plasma oxidation of an elastomeric polymer. *Applied Physics Letters*, 75(17):2557, 1999.

[11] Stefan R Braam and Christine L Mummery. Human stem cell models for predictive cardiac safety pharmacology. *Stem cell research*, 4(3):155–6, May 2010.

[12] Magali Brunet, Terence O$apos$Donnell, Joe O$apos$Brien, Paul McCloskey, and Se$aacute$n Cian $Oacute$ Mathuna. Thick photoresist development for the fabrication of high aspect ratio magnetic coils. *Journal of Micromechanics and Microengineering*, 12(4):444–449, July 2002.

[13] D.K. Cai, a. Neyer, R. Kuckuk, and H.M. Heise. Optical absorption in transparent PDMS materials applied for multimode waveguides fabrication. *Optical Materials*, 30(7):1157–1161, March 2008.

[14] Robert Chang, Jae Nam, and Wei Sun. Direct cell writing of 3D microorgan for in vitro pharmacokinetic model. *Tissue engineering. Part C, Methods*, 14(2):157–66, June 2008.

[15] Sung-Jin Choi, Tae-Hong Kwon, Hwon Im, Dong-Il Moon, David J Baek, Myeong-Lok Seol, Juan P Duarte, and Yang-Kyu Choi. A polydimethylsiloxane (PDMS) sponge for the selective absorption of oil from water. *ACS applied materials & interfaces*, 3(12):4552–6, December 2011.

[16] André Colas. Silicones: Preparation, Properties and Performance. 2005.

[17] Dow Corning. Electronics Sylgard 184 Silicone Elastomer. *Product Datasheet*, pages 1–3, 2013.

[18] R. Dekker, S. Braam, V. Henneken, a. van der Horst, S. Khoshfetrat Pakazad, M. Louwerse, B. van Meer, B. Mimoun, a. Savov, and a. van de Stolpe. Living Chips and Chips for the living. *2012 IEEE Bipolar/BiCMOS Circuits and Technology Meeting (BCTM)*, pages 1–9, September 2012.

[19] Paul M. Dentinger, W.Miles Clift, and Steven H. Goods. Removal of SU-8 photoresist for thick film applications. *Microelectronic Engineering*, 61-62:993–1000, July 2002.

[20] D C Duffy, J C McDonald, O J Schueller, and G M Whitesides. Rapid Prototyping of Microfluidic Systems in Poly(dimethylsiloxane). *Analytical chemistry*, 70(23):4974–84, December 1998.

[21] David T Eddington, Wendy C Crone, and David J Beebe. DEVELOPMENT OF PROCESS PROTOCOLS MATERIAL PROPERTIES. In *Proceedings of Conference on Miniaturized Chemical and Blochemlcal Analysts Systems*, pages 1089–1092, 2003.

[22] M B Esch, T L King, and M L Shuler. The role of body-on-a-chip devices in drug and toxicity studies. *Annual review of biomedical engineering*, 13:55–72, August 2011.

[23] Robert A. (Jr) Freitas. *Nanomedicine, Volume I: Basic Capabilities*. Landes Bioscience, 2003.

[24] D. Fuard, T. Tzvetkova-Chevolleau, S. Decossas, P. Tracqui, and P. Schiavone. Optimization of poly-di-methyl-siloxane (PDMS) substrates for studying cellular adhesion and motility. *Microelectronic Engineering*, 85(5-6):1289–1293, May 2008.

[25] J. Garra, T. Long, J. Currie, T. Schneider, R. White, and M. Paranjape. Dry etching of polydimethylsiloxane for microfluidic systems. *Journal of Vacuum Science & Technology A: Vacuum, Surfaces, and Films*, 20(3):975, 2002.

[26] L. M. Griep, F. Wolbers, B. Wagenaar, P. M. Braak, B. B. Weksler, I. a. Romero, P. O. Couraud, I. Vermes, a. D. Meer, and a. Berg. BBB ON CHIP: microfluidic platform to mechanically and biochemically modulate blood-brain barrier function. *Biomedical Microdevices*, 15(1):145–50, February 2012.

[27] Linda G Griffith and Melody a Swartz. Capturing complex 3D tissue physiology in vitro. *Nature reviews. Molecular cell biology*, 7(3):211–24, March 2006.

[28] Edgar Gutierrez and Alex Groisman. Measurements of elastic moduli of silicone gel substrates with a microfluidic device. *PloS one*, 6(9):e25534, January 2011.

[29] H Hillborg, J F Ankner, U W Gedde, G D Smith, H K Yasuda, and K Wikstro. Crosslinked polydimethylsiloxane exposed to oxygen plasma studied by neutron reflectometry and other surface specific techniques. *Polymer*, 41:6851–6863, 2000.

[30] J. Hong, R. J. Shul, L. Zhang, L. F. Lester, H. Cho, Y. B. Hahn, D. C. Hays, K. B. Jung, S. J. Pearton, C. M. Zetterling, and M. Östling.

Plasma chemistries for high density plasma etching of SiC. *Journal of Electronic Materials*, 28(3):196–201, March 1999.

[31] Yan Huang, Lisha Zheng, Xianghui Gong, Xiaoling Jia, Wei Song, Meili Liu, and Yubo Fan. Effect of cyclic strain on cardiomyogenic differentiation of rat bone marrow derived mesenchymal stem cells. *PloS one*, 7(4):e34960, January 2012.

[32] Dongeun Huh, Geraldine a Hamilton, and Donald E Ingber. From 3D cell culture to organs-on-chips. *Trends in cell biology*, 21(12):745–54, December 2011.

[33] Dongeun Huh, Hyun Jung Kim, Jacob P Fraser, Daniel E Shea, Mohammed Khan, Anthony Bahinski, Geraldine a Hamilton, and Donald E Ingber. Microfabrication of human organs-on-chips. *Nature protocols*, 8(11):2135–57, November 2013.

[34] Jungkyu Kim, Rajesh Surapaneni, and Bruce K Gale. Rapid prototyping of microfluidic systems using a PDMS/polymer tape composite. *Lab on a chip*, 9(9):1290–3, May 2009.

[35] M Liu, S J Skinner, J Xu, R N Han, a K Tanswell, and M Post. Stimulation of fetal rat lung cell proliferation in vitro by mechanical stretch. *The American journal of physiology*, 263(3 Pt 1):L376–83, September 1992.

[36] Miao Liu, Jianren Sun, Ying Sun, Christopher Bock, and Quanfang Chen. Thickness-dependent mechanical properties of polydimethylsiloxane membranes. *Journal of Micromechanics and Microengineering*, 19(3):035028, March 2009.

[37] J C Lötters, W Olthuis, P H Veltink, and P Bergveld. The mechanical properties of the rubber elastic polymer polydimethylsiloxane for sensor applications. *Journal of Micromechanics and Microengineering*, 145(7), 1997.

[38] Alexander Elceario Mag-isa, Bongkyun Jang, Jae-Hyun Kim, Hak-Joo Lee, and Chung-Seog Oh. Coefficient of thermal expansion measurements for freestanding nanocrystalline ultra-thin gold films. *International Journal of Precision Engineering and Manufacturing*, 15(1):105–110, January 2014.

[39] Alvaro Mata, Aaron J Fleischman, and Shuvo Roy. Characterization of polydimethylsiloxane (PDMS) properties for biomedical micro/nanosystems. *Biomedical microdevices*, 7(4):281–93, December 2005.

[40] J Cooper Mcdonald, David C Duffy, Janelle R Anderson, and Daniel T Chiu. Review General Fabrication of microfluidic systems in poly (dimethylsiloxane). *Electrophoresis*, 21:27–40, 2000.

[41] Berend Van Meer. Aligning cardiomyocytes using batch processable techniques, 2010.

[42] Microchem. SU-8 3000 Permanent Epoxy. *Product Datasheet*, 20, 2000.

[43] Microchem. Hardbake of Photoresist Structures. *Application Notes*, 2013.

[44] Eduardo Ortiz. Market withdrawal of Vioxx: is it time to rethink the use of COX-2 inhibitors? *Journal of managed care pharmacy : JMCP*, 10(6):551–4, 2004.

[45] S Khoshfetrat Pakazad, A Savov, S R Braam, and R Dekker. A platform for manufacturable stretchable Micro-Electrode Arrays. In *Eurosensors XXVI*, volume 00. Elsevier, 2012.

[46] S. Khoshfetrat Pakazad, a. M. Savov, a. Van De Stolpe, S. Braam, B. Van Meer, and R. Dekker. A stretchable Micro-Electrode Array for in vitro electrophysiology. *2011 IEEE 24th International Conference on Micro Electro Mechanical Systems*, pages 829–832, 2011.

[47] Saeed Khoshfetrat Pakazad. A Stretchable Multi-Electrode Array (MEA) for cardio-toxicity drug screening applications. Master's thesis, Delft University of Technology, 2010.

[48] Long Que and Yogesh B. Gianchandani. Mechanical properties and pattern collapse of chemically amplified photoresists. *Journal of Vacuum Science & Technology B: Microelectronics and Nanometer Structures*, 18(6):3450, 2000.

[49] John a Rogers, Takao Someya, and Yonggang Huang. Materials and mechanics for stretchable electronics. *Science (New York, N.Y.)*, 327(5973):1603–7, March 2010.

[50] Merja P Ruutu, Xianfeng Chen, Ojas Joshi, Mark a Kendall, and Ian H Frazer. Increasing mechanical stimulus induces migration of Langerhans cells and impairs the immune response to intracutaneously delivered antigen. *Experimental dermatology*, 20(6):534–6, June 2011.

[51] D Sameoto and C Menon. A low-cost, high-yield fabrication method for producing optimized biomimetic dry adhesives. *Journal of Micromechanics and Microengineering*, 19(11):115002, November 2009.

[52] Angel Savov. Etching of Polydimethylsiloxane (PDMS) for Fabrication of Stretchable Micro-Electrode Electrode Arrays, 2012.

[53] Andrea K Smiley, Ã Jennifer M Klingenberg, Ã Bruce J Aronow, Steven T Boyce, Ã W John Kitzmiller, and Dorothy M Supp Ã. Microarray Analysis of Gene Expression in Cultured Skin Substitutes Compared with Native Human Skin. *Journal of Investigative Dermatology*, 125:1286–1301, 2005.

[54] Bauer E. Sumpio, Albert J. Banes, Linda G. Levin, and George Johnson. Mechanical stress stimulates aortic endothelial cells to proliferate. *Journal of Vascular Surgery*, 6(3):252–256, September 1987.

[55] E J Swenson and C Berglund. Scanning the issue. *Proceedings of the IEEE*, 90(10):1611–1613, October 2002.

[56] Ron Unz. Chinese Melamine and American Vioxx: A Comparison. *The American Conservative*, 2012.

[57] M Vlachopoulou, K Tsougeni, K Kontakis, N Vourdas, A Tserepi, and E Gogolides. Plasma etching technology for fabrication and surface modification of plastic microfluidic devices. *Pure and Applied Chemistry*, 86(6), 2010.

[58] Pierre-Jean Wipff, Hicham Majd, Chitrangada Acharya, Lara Buscemi, Jean-Jacques Meister, and Boris Hinz. The covalent attachment of adhesion molecules to silicone membranes for cell stretching applications. *Biomaterials*, 30(9):1781–9, March 2009.

[59] Benjamin C Wood. Skin, Grafts, 2011.

[60] Tony Yeung, Penelope C Georges, Lisa a Flanagan, Beatrice Marg, Miguelina Ortiz, Makoto Funaki, Nastaran Zahir, Wenyu Ming, Valerie Weaver, and Paul a Janmey. Effects of substrate stiffness on cell morphology, cytoskeletal structure, and adhesion. *Cell motility and the cytoskeleton*, 60(1):24–34, January 2005.

[61] Peng Yinsheng, Ye Xiaoling, Xu Bo, Jin Peng, Niu Jiebin, Jia Rui, and Wang Zhanguo. Optimization of inductively coupled plasma etching for low nanometer scale air-hole arrays in two-dimensional GaAs-based photonic crystals. *Journal of Semiconductors*, 31(1):012003, January 2010.

[62] Junying Yu, Maxim a Vodyanik, Kim Smuga-Otto, Jessica Antosiewicz-Bourget, Jennifer L Frane, Shulan Tian, Jeff Nie, Gudrun a Jonsdottir, Victor Ruotti, Ron Stewart, Igor I Slukvin, and James a Thomson. Induced pluripotent stem cell lines derived from human somatic cells. *Science (New York, N.Y.)*, 318(5858):1917–20, December 2007.

[63] D. Zhuang and J.H. Edgar. Wet etching of GaN, AlN, and SiC: a review. *Materials Science and Engineering: R: Reports*, 48(1):1–46, January 2005.

Acknowledgements

Aangezien een ingenieur maar een ingenieur is, was het waanzinnig leerzaam om samen te werken met het Medisch Centrum van de Vrije Universiteit te Amsterdam. De open houding jegens multidisciplinair onderzoek zorgt voor een waardevolle en interessante samenwerking met professor Sue Gibbs en haar onderzoeksgroep. Extra veel dank gaat uit naar Taco Waaijman, die mij heeft geholpen om de anatomie van de huid te begrijpen, het Cytostretch model te valideren en daar precies op tijd prachtige kleuringen van te maken.

De nauwe samenwerking met Philips is ook waardevol gebleken. Bij deze wil ik Hans Kroes bedanken voor het laseren van PDMS. Veel dank gaat ook uit naar Angel Savov and to Saeed Khoshfetrat Pazakad, for sharing their knowledge and thinking together with me towards solutions. Ook Anja van der Stolpe wil ik bedanken voor haar eindeloze enthousiasme en aanmoedigingen.

Het meeste werk is verzet bij het Delft Institute for Microsystems and Nanoelectronics (DIMES) en daar zou helemaal niks mogelijk zijn zonder de DIMES Staff. Hun expertise and hulpvaardigheid heeft het werken in de cleanroom erg leerzaam en prettig gemaakt. Also, to all the PhD and MSc students that are always willing to help; thank you a lot!

Charlotte van Meer wil ik hartelijk bedanken voor haar hulp tijdens met schrijven van deze thesis, ondanks haar overvolle agenda.

Gregory "Chief" Pandraud, je te remercie beaucoup de ton aide, tu m'as appris bien des choses. C'tait un plaisir de travailler avec toi.

Tot slot, Ronald Dekker, zonder jou had ik dit onderzoek nooit gedaan. Jij hebt mij enthousiast gemaakt voor onderzoek met leuke projecten en creatieve brainstormsessies. Veel dank voor het vertrouwen en de verantwoordelijkheid die je tijdens jouw begeleiding gaf, ik heb veel van je geleerd, al sinds 2010!